

---

# DOUBLY ROBUST IDENTIFICATION OF TREATMENT EFFECTS FROM MULTIPLE ENVIRONMENTS

**Anonymous authors**

Paper under double-blind review

## ABSTRACT

Practical and ethical constraints often dictate the use of observational data for causal inference, particularly in medicine and social sciences. Yet, observational datasets are prone to confounding, potentially compromising the validity of conclusions. While adjusting for all available covariates is a common corrective strategy, this approach can introduce bias, especially when post-treatment variables are present or some variables remain unobserved—a frequent scenario in practice. Avoiding this bias often requires detailed knowledge of the underlying causal graph, a challenging and often impractical prerequisite. In this work, we propose RAMEN, an algorithm that tackles this challenge by leveraging the heterogeneity of multiple data sources without the need to know the complete causal graph. Notably, RAMEN achieves *doubly robust identification*: we identify the treatment effect if either the causal parents of the treatment or those of the outcome are observed. Empirical evaluations across synthetic, semi-synthetic, and real-world datasets show that our approach significantly outperforms existing methods.

## 1 INTRODUCTION

Estimating treatment effects is a key objective in fields such as medicine and social sciences, as it helps determine the impact of interventions like novel treatments or policies. To achieve this goal, researchers often use randomized controlled trials since randomizing the treatment assignment guarantees unbiased treatment effect estimates under mild assumptions. However, methods relying on randomized data face several issues, such as small sample sizes, sample populations that do not reflect those seen in the real world, and ethical or financial constraints. As a result, there is growing interest in using observational data to infer causal relationships when randomized data is scarce.

A fundamental challenge in using observational data is selecting a *valid adjustment set*, i.e. a set of covariates that can be used to correctly identify the treatment effect (Hernán & Robins, 2010, Chapter 7). Practitioners often adjust for all available covariates (Austin, 2011), but this approach runs the risk of including *bad controls*—covariates that open backdoor paths between the treatment ( $T$ ) and the outcome ( $Y$ ), thereby introducing bias into the treatment effect estimate (Rosenbaum, 1984). For instance, consider the causal graphs illustrated in Figure 1. Is  $\{X_1, X_2\}$  always a valid adjustment set? In Figure 1a,  $\{X_1, X_2\}$  blocks all backdoor paths, allowing for treatment effect identification, whereas including  $X_1$  in Figure 1b opens a backdoor path, introducing bias in the treatment effect estimate. Hence, blindly including all covariates in the adjustment set is not always a valid strategy.

Although the example above might seem artificial, bad controls pose a significant challenge, especially in the social sciences, where the causal ordering of the observed covariates is often not clear (King, 2010; Montgomery et al., 2018). For instance, Acharya et al. (2016) found that up to two-thirds of empirical studies in political science that make causal claims inadvertently include bad controls in their analysis, leading to biased estimates of the treatment effects. In a first attempt to address this challenge in a data-driven manner, Shi et al. (2021) leverage access to multiple heterogeneous data sources—a common scenario in practice, e.g. think of observational studies from different countries—to develop a method that identifies the treatment effect in the presence of post-treatment variables. However, their approach fails when not all the variables in the causal graph are

054  
055  
056  
057  
058  
059  
060  
061  
062  
063  
064  
065  
066  
067  
068  
069  
070  
071  
072  
073  
074  
075  
076  
077  
078  
079  
080  
081  
082  
083  
084  
085  
086  
087  
088  
089  
090  
091  
092  
093  
094  
095  
096  
097  
098  
099  
100  
101  
102  
103  
104  
105  
106  
107

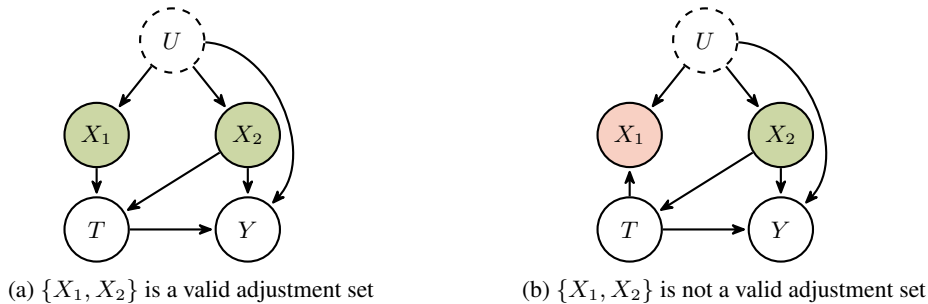


Figure 1: Two causal graphs illustrating when the set of all covariates is or is not a valid adjustment set: (a)  $\{X_1, X_2\}$  blocks all backdoor paths between  $T$  and  $Y$ , making it a valid adjustment set; (b)  $X_1$  opens a backdoor path between  $T$  and  $Y$ , introducing bias in the treatment effect estimate if adjusted for. Unobserved variables are dashed and colored in white, bad controls are colored in red, and good controls are colored in green.

observed, and the distribution of the unobserved variables shifts across environments, e.g. in the setting of Figure 1b.

In this work, we propose **Robust ATE** identification from **Multiple ENvironments** (RAMEN), an algorithm that addresses this challenge by leveraging the heterogeneity of multiple data sources without the need to know or learn the complete causal graph. Notably, our algorithm achieves *doubly robust identification*: we identify the treatment effect if either the causal parents of the treatment or those of the outcome are observed. In particular, our approach combines two identification strategies—one based on the parents of the treatment and the other on the parents of the outcome—allowing identification even when some variables remain unobserved, as in Figure 1b, where previous methods fail. Our key contributions are outlined below.

- We introduce a novel double robustness property, which targets identification rather than estimation. We then provide the first, to our knowledge, doubly robust identification guarantees for treatment effect in the presence of both post-treatment and unobserved variables.
- We propose two novel algorithms that satisfy our double robustness property. The first uses a combinatorial search over subsets of covariates, while the second uses the Gumbel trick to enable a scalable optimization procedure. Additionally, we introduce a novel kernel invariance loss, which may be of independent interest for domain generalization.
- We demonstrate that our algorithms significantly outperform existing approaches for treatment effect estimation in the presence of post-treatment variables on synthetic and semi-synthetic datasets. We further evaluate our method on a real-world example, showing that our results align with established epidemiological knowledge.

## 2 RELATED WORK

Various criteria and methods have been proposed for the purpose of covariate selection, often in the form of necessary and sufficient conditions for a given causal graph, such as the backdoor criterion and its variations (Pearl, 1995; Shpitser et al., 2010; Vander Weele & Shpitser, 2011; Maathuis & Colombo, 2015; Perković et al., 2018). However, since the causal graph is rarely known in real-world applications, the most common approach assumes that all observed covariates are pre-treatment and includes all of them (Austin, 2011, p. 414). Yet, this strategy has several drawbacks: including certain pre-treatment covariates can introduce M-bias (Entner et al., 2013; Gultchin et al., 2020; Cheng et al., 2022b; Shah et al., 2022), and even when bias is not an issue, selecting a smaller subset of covariates leads to more efficient estimates (Hahn, 2004; White & Lu, 2011; De Luna et al., 2011; Rotnitzky & Smucler, 2020; Witte et al., 2020; Henckel et al., 2022; Guo et al., 2023).

The problems described above are orthogonal to our focus in this paper, which is on scenarios where both post-treatment and unobserved variables are present (see Appendix B for a more comprehen-

sive literature review). In this context, previous works have achieved partial identification, albeit with significant computational costs (Hytinen et al., 2015; Malinsky & Spirtes, 2017). More recently, Cheng et al. (2022a) achieved exact identification using an anchor variable. However, anchor variables and multiple environments are distinct settings, each applicable under different conditions and not directly comparable. To our knowledge, our work is the first to achieve point identification in the presence of both post-treatment and unobserved variables using multiple environments.

Finally, our double robustness property significantly differs from most classic results in the existing literature (Robins et al., 1994; Vansteelandt et al., 2008; Chernozhukov et al., 2018). The key distinction is that our property targets identification rather than estimation. Some previous work has achieved similar robust identification results in the context of panel data (Arkhangelsky & Imbens, 2022) and instrumental variables (Kang et al., 2016; Hartwig et al., 2017; Guo et al., 2018; Kuang et al., 2020; Hartford et al., 2021)—usually by assuming that only a fraction of the available instruments are valid. However, to our knowledge, we are the first to achieve doubly robust identification in the context of post-treatment and unobserved variables when valid instruments are not available.

### 3 PROBLEM SETTING

We assume the data is collected under different experimental conditions, represented by environments  $e \in \mathcal{E}$ , with  $|\mathcal{E}| = n_e$ . For each environment  $e \in \mathcal{E}$ , we have access to a dataset  $D^e = \{(X_i, T_i, Y_i)\}_{i=1}^n$  which contains  $n$  i.i.d. tuples sampled from the marginal induced by the joint distribution  $(X, U, T, Y) \sim \mathbb{P}^e$ , where  $X \in \mathbb{R}^d$  are the observed covariates,  $U \in \mathbb{R}^k$  are unobserved covariates,  $T \in \{0, 1\}$  is a binary treatment assignment variable and  $Y \in \mathbb{R}$  is the observed outcome. We denote by  $\mathbb{P} = \frac{1}{|\mathcal{E}|} \sum_{e \in \mathcal{E}} \mathbb{P}^e$  the joint distribution of the pooled environments.

#### 3.1 CAUSAL INFERENCE PRELIMINARIES

For a fixed directed acyclic graph (DAG)  $\mathcal{G}$ , we denote the complete set of its nodes by  $\tilde{Z}$  and only the *observed* nodes by  $Z$ . We denote the index set of parents, ancestors, and descendants for any node  $\tilde{Z}_i$  by  $\text{Pa}(\tilde{Z}_i)$ ,  $\text{An}(\tilde{Z}_i)$ , and  $\text{De}(\tilde{Z}_i)$ , respectively. Additionally, for any subset  $S \subseteq [p]$ ,  $\tilde{Z}_S$  denotes the subvector of  $\tilde{Z}$  corresponding to the indices in  $S$ . In what follows, we formally assume that, for all the experimental settings, the joint distribution  $\mathbb{P}^e$  is generated according to a structural causal model (Aldrich, 1989) induced by a DAG  $\mathcal{G}$ .

**Assumption 3.1** (Data distribution). *For each environment  $e \in \mathcal{E}$ , the distribution  $\mathbb{P}^e$  is induced by a structural causal model (SCM), defined as a tuple  $\mathcal{M}^e = (\mathcal{G}, \{f_i^e\}_{i=1}^p, \mathbb{P}_\epsilon^e)$  on  $p = d + k + 2$  variables  $(\tilde{Z}_1, \dots, \tilde{Z}_p)$ , where the observed covariates are  $X = \tilde{Z}_{[d]}$ , the unobserved covariates are  $U = \tilde{Z}_{d+[k]}$ , the treatment variable is  $T = \tilde{Z}_{p-1}$ , and the outcome variable is  $Y = \tilde{Z}_p$ , with  $p \notin \text{An}(T)$ . The SCM defines the probability distribution  $\mathbb{P}^e$  by setting for each  $j \in [p]$*

$$\tilde{Z}_j \leftarrow f_j^e(\tilde{Z}_{\text{Pa}(\tilde{Z}_j)}, \epsilon_j), \quad j = 1, \dots, p,$$

where  $f_j^e : \mathbb{R}^p \times \mathbb{R} \rightarrow \mathbb{R}$  is a measurable function and  $\epsilon \in \mathbb{R}^p$  is an exogenous noise vector following the joint distribution  $\mathbb{P}_\epsilon^e$  over  $p$  independent variables.

Further, along the lines of the existing methods in the literature (Shi et al., 2021; Wang et al., 2023), we require the absence of observed mediators between  $T$  and  $Y$  in the structural causal model.

**Assumption 3.2** (Absence of Mediators). *We assume that no observed mediators exist between  $T$  and  $Y$ , i.e. it holds that*

$$\text{De}(T) \cap \text{An}(Y) \cap [d] = \emptyset.$$

We remark that Assumption 3.2 is *falsifiable* using statistical tests to determine whether a covariate is a mediator between  $T$  and  $Y$  (see, e.g. Baron & Kenny (1986); Preacher & Hayes (2004)). Further, note that when this assumption is violated, the identified causal quantity corresponds to the natural direct effect (Pearl, 2022), which is still a quantity of separate interest in fields like epidemiology (Tchetgen & VanderWeele, 2014) and social sciences (Imai et al., 2011).

---

### 3.2 TREATMENT EFFECT IDENTIFICATION

Our goal is to identify the treatment effects for different environments in the presence of unobserved and post-treatment variables. More specifically, we are interested in the average treatment effects (ATEs) for all environments  $e \in \mathcal{E}$ , defined as

$$\theta^e = \mathbb{E}_{\mathbb{P}^e} \left[ Y^{\text{do}(T=1)} - Y^{\text{do}(T=0)} \right].$$

A common approach for identifying the ATE is to find a *valid adjustment set* (Shpitser et al., 2010), that is, a subset  $S \subseteq [d]$  of the covariates that satisfies both the classic outcome and treatment identification formulae, i.e. for all environments  $e \in \mathcal{E}$  and  $t \in \{0, 1\}$  it holds that

$$\mathbb{E}_{\mathbb{P}^e} \left[ Y^{\text{do}(T=t)} \right] = \mathbb{E}_{\mathbb{P}^e} \left[ \mathbb{E}_{\mathbb{P}^e} [Y \mid X_S, T = t] \right] \text{ and } \mathbb{E}_{\mathbb{P}^e} \left[ Y^{\text{do}(T=t)} \right] = \mathbb{E}_{\mathbb{P}^e} \left[ \frac{Y \mathbb{I}\{T = t\}}{\mathbb{P}^e(T = t \mid X_S)} \right]. \quad (1)$$

Several criteria have been proposed in the literature to find valid adjustment sets, with the backdoor criterion being the most prominent—see Peters et al. (2017, Sec. 6.6) for a detailed discussion. However, these criteria crucially rely on knowledge of the underlying causal graph—a challenging and often impractical prerequisite. Therefore, it is commonly assumed among practitioners that the set  $S$  of all covariates is a valid adjustment set, which is a reasonable assumption only in settings where all the observed covariates are pre-treatment.

In contrast, our work focuses on settings where both post-treatment and unobserved covariates are present. To identify the ATE in such settings, we need to introduce two key assumptions. More formally, we allow each environment to have a different joint distribution  $\mathbb{P}^e$  over  $(X, U, Y, T)$ . However, we assume that there exists an invariant node, either  $T$  or  $Y$ , such that its parents are fully observed and the conditional mean of the node given its parents is invariant across environments.

**Assumption 3.3** (Invariant node). *We assume that one of the following holds for all  $e \in \mathcal{E}$ :*

- (a)  $\text{Pa}(T)$  are observed and  $\mathbb{E}_{\mathbb{P}^e} [T \mid Z_{\text{Pa}(T)}] = \mathbb{E}_{\mathbb{P}} [T \mid Z_{\text{Pa}(T)}]$ ,  $\mathbb{P}^e - a.s.$
- (b)  $\text{Pa}(Y)$  are observed and  $\mathbb{E}_{\mathbb{P}^e} [Y \mid Z_{\text{Pa}(Y)}] = \mathbb{E}_{\mathbb{P}} [Y \mid Z_{\text{Pa}(Y)}]$ ,  $\mathbb{P}^e - a.s.$

We denote the node  $V \in \{T, Y\}$  for which the above holds as the **invariant node**  $V_{\text{inv}}$ .

It is worth emphasizing that each of the above assumptions can provide identification of the ATE on its own. Here, we combine these two identification assumptions to obtain doubly robust identification: we only require that either (a) or (b) in Assumption 3.3 holds. This is similar in spirit to the double robustness literature (Robins & Rotnitzky, 1995; Chernozhukov et al., 2018), where only one of two assumptions about model specification needs to hold to obtain valid ATE estimates. We discuss the differences with the classic double robustness literature in Section 4.

Further, the invariance assumptions (a) and (b) are closely related to the conditions in the invariance-based domain generalization literature, such as Peters et al. (2016); Rojas-Carulla et al. (2018); Gu et al. (2024). While these settings are included in Assumption 3.3 (as we discuss in Appendix A.1), our setting does not require full independence of the noise variable<sup>1</sup>, unlike Peters et al. (2016), nor is it limited to the additive noise case, as in Gu et al. (2024), which is does not hold in the case of binary treatment variables.

Finally, we comment on the observability part of Assumption 3.3: assuming  $\text{Pa}(V_{\text{inv}})$  are observed is strictly weaker than causal sufficiency, where the full causal graph is assumed to be observed. Specifically, we allow for some unobserved variables, such as the path  $U \rightarrow Y$  in Figures 1a and 1b, for which Assumption 3.3 still holds. In contrast, Shi et al. (2021) assume that there are no unobserved variables to identify the treatment effect, and if some parents of  $Y$  remain unobserved, the treatment effect estimates from their algorithm would not be valid.

---

<sup>1</sup>Although we require independence of exogenous noise variables in Assumption 3.1 for the *full* graph, here, we refer to the graph limited to the observed nodes, where the noise variables  $\epsilon_V$  can be dependent on  $\text{Pa}(V)$ .

---

## 4 METHODOLOGY

In this section, we introduce RAMEN, our method to identify the ATE by leveraging the heterogeneity in the observed data. First, we present a doubly robust population-level estimator and discuss under which conditions it equals to the ATE. Then, we show how to compute this estimator tractably by minimizing a novel invariance loss and propose two algorithms to do so: a combinatorial search over subsets and a more scalable differentiable approach for high-dimensional covariate settings.

### 4.1 POPULATION-LEVEL ESTIMATOR

In what follows, we denote by  $\mathcal{I} = [d] \cup \{p-1, p\}$  the index set corresponding to the observed variables  $Z := (X_{[d]}, T, Y)$ . For any node  $V \in \{T, Y\}$  and any observed subset  $S \subseteq \mathcal{I} \setminus V$ , we define the conditional means over the pooled and individual environments

$$\bar{m}_S(Z; V) := \mathbb{E}_{\mathbb{P}}[V \mid Z_S] \quad \text{and} \quad m_S^e(Z; V) := \mathbb{E}_{\mathbb{P}^e}[V \mid Z_S].$$

We begin by observing that, by Assumption 3.3, there exists an invariant node  $V_{\text{inv}} \in \{T, Y\}$  and a subset of covariates  $S$  (given by, e.g.,  $\text{Pa}(V_{\text{inv}})$ ), for which the following conditional moment constraint holds for all environments  $e \in \mathcal{E}$

$$\exists S \subseteq \mathcal{I} \setminus V_{\text{inv}} : m_S^e(Z; V_{\text{inv}}) = \bar{m}_S(Z; V_{\text{inv}}), \mathbb{P}^e - \text{a.s.} \quad (2)$$

The set  $S$  is not necessarily unique: besides the (observed) parents of  $V_{\text{inv}}$  for instance, the invariance could also hold for certain supersets of  $\text{Pa}(V_{\text{inv}})$ . Denote as  $L^0(\mathbb{R}^d)$  the space of measurable functions over  $\mathbb{R}^d$ . By observing that the conditional moment constraint above is equivalent to the following infinite set of unconditional moment constraints

$$\mathbb{E}_{\mathbb{P}^e}[(V_{\text{inv}} - \bar{m}_S(Z; V_{\text{inv}}))h(Z_S)] = 0, \quad \text{for all } h \in L^0(\mathbb{R}^{|S|}), \quad (3)$$

any set  $S$  that satisfies the invariance constraint Equation (2) is also contained in

$$\underset{S \subseteq \mathcal{I} \setminus V_{\text{inv}}}{\text{argmin}} \max_{e \in \mathcal{E}} \left( \sup_{h \in L^0(\mathbb{R}^{|S|})} \mathbb{E}_{\mathbb{P}^e}[(V_{\text{inv}} - \bar{m}_S(Z; V_{\text{inv}}))h(Z_S)] \right)^2 := \underset{S \subseteq \mathcal{I} \setminus V_{\text{inv}}}{\text{argmin}} J_S(Z; V_{\text{inv}}).$$

However, since the invariant node  $V_{\text{inv}}$  is not known beforehand, we search for a set of observed nodes that satisfy the invariance with respect to either  $T$  or  $Y$ , that is, we want to find

$$S_{\text{opt}} \in \underset{S \subseteq \mathcal{I} \setminus V}{\text{argmin}} \min_{V \in \{T, Y\}} J_S(Z; V). \quad (4)$$

Let us define the pooled conditional outcome and treatment functions as  $\bar{\mu}_t(X_{S_{\text{opt}}}) := \mathbb{E}_{\mathbb{P}}[Y \mid X_{S_{\text{opt}}}, T = t]$  and  $\bar{\pi}(X_{S_{\text{opt}}}) := \mathbb{E}_{\mathbb{P}}[T \mid X_{S_{\text{opt}}}]$ . For a minimizer  $S_{\text{opt}}$ , we then define the corresponding population-level RAMEN estimator for all environments  $e \in \mathcal{E}$  as

$$\theta_{\mathfrak{S}}^e(S_{\text{opt}}) := \mathbb{E}_{\mathbb{P}^e} \left[ \bar{\mu}_1(X_{S_{\text{opt}}}) - \bar{\mu}_0(X_{S_{\text{opt}}}) + \frac{(Y - \bar{\mu}_1(X_{S_{\text{opt}}}))T}{\bar{\pi}(X_{S_{\text{opt}}})} - \frac{(Y - \bar{\mu}_0(X_{S_{\text{opt}}}))(1-T)}{1 - \bar{\pi}(X_{S_{\text{opt}}})} \right]. \quad (5)$$

We remark here that using  $\theta_{\mathfrak{S}}^e$  allows us to estimate the treatment and outcome functions from the pooled data and—in the finite sample setting—benefit from a much larger sample size. In the following Section 4.2, we show that under sufficient data heterogeneity, detailed in Assumption 4.1, our population-level estimator  $\theta_{\mathfrak{S}}^e$  is equivalent for all  $S_{\text{opt}}$  in Equation (4) and equal to the true treatment effect. In Sections 4.3 and 4.4, we then discuss how we can use (5) to find a good finite-sample ATE estimate in a computationally efficient way.

### 4.2 DOUBLY ROBUST IDENTIFICATION

Without further assumptions, finding the minimizer of Equation (4) is not sufficient for identifying the ATE via (5): for instance, if there is no variability between distributions  $\mathbb{P}^e$ , our objective could be trivially minimized by any observed subset  $S$ . Only when there is “enough” heterogeneity in the observed environments, will  $\theta_{\mathfrak{S}}^e$  result in an unbiased estimate of the ATE. We formalize this condition in the following assumption.

**Assumption 4.1** (Identification condition). For all  $V \in \{T, Y\}$  and  $S \subset \mathcal{I} \setminus V$ , it holds that:

$$\bar{\mathbb{P}}(\bar{m}_S(Z; V) \neq \bar{m}_{\text{Pa}(V)}(Z; V)) > 0 \implies \exists e \in \mathcal{E} : \mathbb{P}^e(m_S^e(Z; V) \neq \bar{m}_S(Z; V)) > 0.$$

Assumption 4.1 can be understood as ensuring that the environments present sufficient heterogeneity. This heterogeneity guarantees that conditioning on any set  $S$  with invariant outcome or treatment functions across environments (i.e., a set identified by our method) is equivalent to conditioning on the parents. Conversely, this assumption prevents the discovery of “bad” sets  $S$  during our minimization procedure in Equation (4). Although our environment variability assumption is relatively strict, it is a common requirement in the invariance literature (cf. Peters et al. (2016); Arjovsky et al. (2019)). For example, in the simultaneous noise intervention setting described in Peters et al. (2016, Section 4.2.3), Assumption 4.1 can be satisfied with as few as two environments. Further, in the case of single-node interventions, Assumption 4.1 requires approximately  $\mathcal{O}(p)$  environments.

We now present our formal identification result for the ATE.

**Theorem 1** (Doubly robust identification). Let  $S_{\text{opt}}$  be any minimizer of the invariance loss, i.e.

$$S_{\text{opt}} \in \operatorname{argmin}_{S \subseteq \mathcal{I} \setminus V} \min_{V \in \{T, Y\}} J_S(Z; V). \quad (6)$$

Then, under Assumptions 3.2, 3.3, 4.1, if positivity holds, that is  $e \in \mathcal{E}$

$$\forall e \in \mathcal{E} : \mathbb{P}^e(T = t \mid X_{S_{\text{opt}}} = x) > 0, \forall t \in \{0, 1\} \text{ and } \forall x \in \operatorname{supp}(\mathbb{P}_X^e),$$

we can identify the treatment effect, i.e.  $\forall e \in \mathcal{E} : \theta^e = \theta_{\ominus}^e(S_{\text{opt}})$ .

The positivity assumption is standard in the literature—see e.g. Hernán & Robins (2010, Sec. 3.2)—and widely known to be necessary for identifying the treatment effect in observational studies. Theorem 1 states that any solution to our invariance loss is a valid adjustment set in the sense that it is sufficient to identify the average treatment effect in all the environments. In contrast, classical double robustness literature (Robins et al., 1994; Vansteelandt et al., 2008; Chernozhukov et al., 2018) assumes prior knowledge of a valid adjustment set  $S$  that makes the ATE identifiable, whereas our goal in this paper is to find such a set  $S$ .

### 4.3 KERNELIZED INVARIANCE LOSS

A major problem of the loss function in Equation (4) is that it is computationally infeasible to search over the entire space of measurable functions. However, we can simplify the problem by restricting  $h$  to be in a reproducing kernel Hilbert space (RKHS), and as long as the reproducing kernel of the RKHS is universal (e.g. Gaussian kernel), the two formulations are equivalent (Gretton et al., 2012). More formally, for any subset  $S \subseteq \mathcal{I} \setminus V$  and environment  $e \in \mathcal{E}$ , we can write

$$\begin{aligned} \left( \sup_{h \in L^0(\mathbb{R}^{|S|})} \mathbb{E}_{\mathbb{P}^e} \left[ \underbrace{(V - \bar{m}_S(Z; V)) h(Z_S)}_{:= \delta_S(Z, V)} \right] \right)^2 &= \left( \sup_{\|h\|_{\mathcal{H}} \leq 1} \mathbb{E}_{\mathbb{P}^e} [\delta_S(Z, V) h(Z_S)] \right)^2 \\ &= \|\mathbb{E}_{\mathbb{P}^e} [\delta_S(Z, V) k(\cdot, Z_S)]\|_{\mathcal{H}}^2 \\ &= \mathbb{E}_{\mathbb{P}^e} [\delta_S(Z, V) k(Z_S, Z'_S) \delta_S(Z', V')], \end{aligned}$$

where  $k$  is a uniformly bounded reproducing kernel corresponding to a universal RKHS  $\mathcal{H}$  (Steinwart, 2001, Definition 4), and  $(V', Z')$  is an independent copy of  $(V, Z)$  following the same distribution. Hence, we can rewrite our loss in a closed-form solution as

$$J_S(Z; V) = \max_{e \in \mathcal{E}} \mathbb{E}_{\mathbb{P}^e} [\delta_S(Z, V) k(Z_S, Z'_S) \delta_S(Z', V')]. \quad (7)$$

**Relation to existing invariance losses** Starting from the work of Peters et al. (2016), there is considerable literature proposing methods to estimate invariant predictors, especially when the optimal predictor is linear. These methods broadly fall into two categories: hypothesis test-based methods (Peters et al., 2016; Heinze-Deml et al., 2018; Pfister et al., 2019) and optimization-based

methods (Arjovsky et al., 2019; Ghassami et al., 2017; Rothenhäusler et al., 2019; 2021; Pfister et al., 2021; Yin et al., 2024; Shen et al., 2023; Gu et al., 2024). Our approach falls in the latter category, with a fundamental distinction. While all these works utilize the invariance principle to improve prediction in unseen environments and generalize to new settings, our goal is to identify a treatment effect in known environments. This is reflected in our loss function, as it does not measure the quality of the predictor in any way—e.g. using a least squares loss. Nonetheless, our invariance loss could also be of interest in the domain generalization literature as it retains the benefits of the invariance loss in Gu et al. (2024) while significantly simplifying their optimization procedure.

#### 4.4 A FULLY DIFFERENTIABLE LOSS

In some cases, searching over all possible subsets of covariates is computationally infeasible. To address this, we propose a continuous relaxation of the optimization problem that can be efficiently solved using gradient descent. Specifically, we select the nodes as  $Z_w := B(w) \odot Z$ , where the  $j$ -th component of  $B(w) \in \{0, 1\}^{d+1}$  is sampled independently from a Bernoulli distribution with success probability  $\text{sigmoid}(w_j)$ . We then aim to solve the following optimization problem:

$$w^{\text{opt}} \in \underset{w \in \mathbb{R}^{d+1}}{\text{argmin}} \quad \min_{\theta \in \mathbb{R}^{d+1}, V \in \{T, Y\}} \max_{e \in \mathcal{E}} \mathbb{E}_{\mathbb{P}^{e, B(w)}} [(V - f_\theta(Z_w))k(Z_w, Z'_w)(V' - f_\theta(Z'_w))],$$

where  $f_\theta$  is a neural network parametrized by  $\theta$ . Since the weights are discrete, direct differentiation is not possible. To overcome this, we use a Gumbel approximation (Jang et al., 2017; Maddison et al., 2017), where the  $j$ -th component of  $B(w)$  is approximated as:

$$B_j(w) \approx \text{sigmoid} \left( \frac{w_j + G_{1,j} - G_{2,j}}{\tau} \right), \quad \text{as } \tau \rightarrow 0^+,$$

with  $G_{1,j}$  and  $G_{2,j}$  being  $\text{Gumbel}(0, 1)$  random variables. This approximation makes  $B(w)$  differentiable (where it was previously discontinuous in  $w_j$ ), allowing us to optimize using gradient descent while gradually annealing the hyperparameter  $\tau$ . Finally, we construct the subset of covariates  $S_{\text{opt}}$  by including  $Z_i$  only if the weights are positive, that is  $S_{\text{opt}} = \{i : w_i^{\text{opt}} > 0\}$ . We refer the reader to Appendix A.3 for the complete implementation details of our algorithms.

## 5 EXPERIMENTS

In this section, we evaluate our method through experiments on synthetic, semi-synthetic, and real-world data. We first present experiments on several known DAGs, where the invariances are known and satisfy our assumptions. In line with our theory, RAMEN correctly identifies the ATE, resulting in a low estimation error, whereas other methods tend to fail. We also test RAMEN on a more challenging benchmark by uniformly sampling DAGs using the Erdős–Rényi model—a standard approach for testing causal methods across a wide variety of graph topologies (Huang et al., 2020). Finally, we validate our estimator beyond purely synthetic data: first in a semi-synthetic setting with real-world covariates and then in a real-world setting where we compare the conclusions from RAMEN with established epidemiological findings.

In our experiments, we focus on the statistical task of estimating the average treatment effect (ATE)  $\theta^e$  for each environment  $e \in \mathcal{E}$ . To evaluate the performance of an estimator  $\hat{\theta}^e$ , we compute the mean absolute error (MAE) averaged across environments:  $\frac{1}{|\mathcal{E}|} \sum_{e \in \mathcal{E}} |\theta^e - \hat{\theta}^e|$ . We evaluate two implementations of RAMEN: (i)  $\hat{\theta}_\oplus$ , based on combinatorial subset search (Section 4.3), and (ii)  $\hat{\theta}_{\text{insta-}\oplus}$ , based on the Gumbel trick (Section 4.4). We compare our algorithms against three baselines:  $\hat{\theta}_{\text{irm}}$ , the IRM approach for treatment effect estimation proposed by Shi et al. (2021);  $\hat{\theta}_{\text{all}}$ , which adjusts for all available covariates; and  $\hat{\theta}_{\text{null}}$ , which does not adjust for any covariates.

### 5.1 SYNTHETIC EXPERIMENTS WITH KNOWN DAGS

We start with data generated from distributions with simple underlying DAGs that satisfy our invariance assumptions, as illustrated in Figure 2 (Row 2). Most importantly, we consider three distinct

378  
379  
380  
381  
382  
383  
384  
385  
386  
387  
388  
389  
390  
391  
392  
393  
394  
395  
396  
397  
398  
399  
400  
401  
402  
403  
404  
405  
406  
407  
408  
409  
410  
411  
412  
413  
414  
415  
416  
417  
418  
419  
420  
421  
422  
423  
424  
425  
426  
427  
428  
429  
430  
431

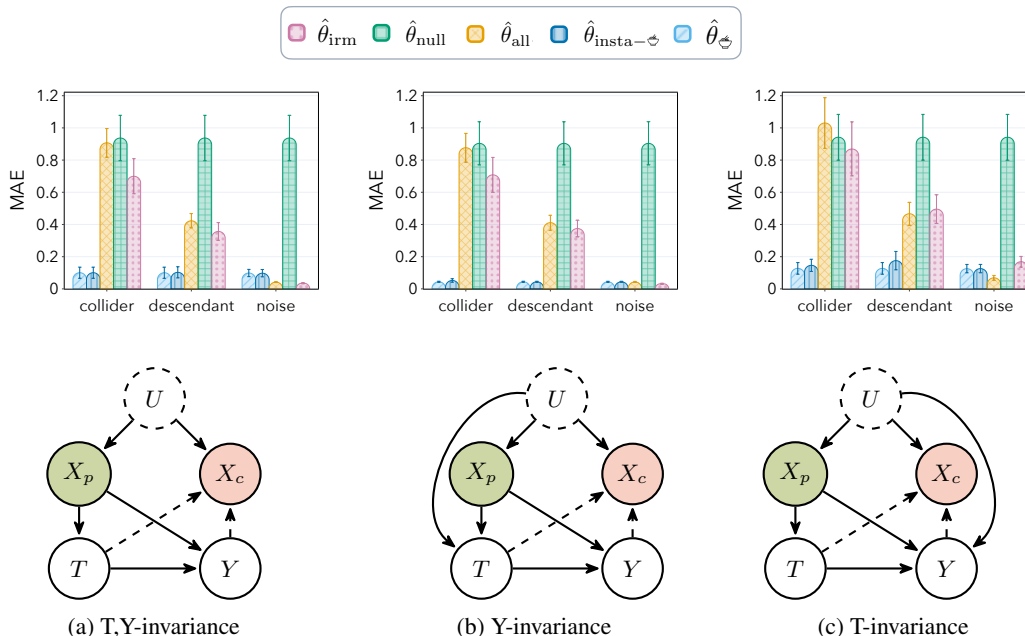


Figure 2: **(Row 1)** For all the plots:  $n = 2500$ ,  $d = 3$ ,  $|\mathcal{E}| = 5$ . We plot the mean absolute error averaged across environments when: (a) both invariances are preserved; (b) the invariance w.r.t  $Y$  is preserved; (c) the invariance w.r.t  $T$  is preserved. We report mean and standard error over 20 runs. **(Row 2)** Graphical models that capture our data generating process: (a)  $U$  does not break any invariance; (b)  $U$  breaks the invariance between  $X_p$  and  $T$ ; (c)  $U$  breaks the invariance between  $X_p$  and  $Y$ . Dashed nodes are unobserved, and dashed lines denote optional edges.

scenarios<sup>2</sup>: (a) Y and T-invariances, i.e. both (a) and (b) in Assumption 3.3 hold; (b) Y-invariance, i.e. only Assumption 3.3 (b) holds; (c) T-invariance, i.e. only Assumption 3.3 (a) holds. For each of the three different invariance scenarios, we further consider three variants: where  $X_c$  is either a descendant of  $Y$ , a collider between  $T$  and  $Y$ , or independent noise. For each of these cases, treatment effects are fixed, and coefficients are sampled from a standard normal distribution. For a description of the complete data-generating process, please refer to Appendix D.1. From theory, we expect that:  $\hat{\theta}_{\text{null}}$  should always be biased since there is a confounder between  $T$  and  $Y$ ;  $\hat{\theta}_{\text{all}}$  should be biased only when  $X_c$  is a collider or a descendant;  $\hat{\theta}_{\text{irm}}$  should be biased only in the T-invariance case;  $\hat{\theta}_{\leftrightarrow}$  and  $\hat{\theta}_{\text{insta-}\leftrightarrow}$  should never be biased in these settings.

In Figure 2 (Row 1), we present the empirical MAE for all methods, and we confirm the predictions from theory. Our methods,  $\hat{\theta}_{\leftrightarrow}$  and  $\hat{\theta}_{\text{insta-}\leftrightarrow}$ , consistently achieve lower MAE compared to the baselines in all scenarios, indicating that the differentiable relaxation of our method does not significantly compromise statistical performance. Expectedly, for T-invariance, the performance of  $\hat{\theta}_{\text{irm}}$  deteriorates markedly—even in scenarios where the post-treatment variable is independent noise, it performs worse than simply adjusting for all available covariates. In contrast, our approach remains robust even when one of the invariances is compromised. Finally, we observe that relying on T-invariance leads to increased error across methods since the adjustment set we recover, the parents of the treatment, is not statistically efficient, see e.g. Henckel et al. (2022, Corollary 3.4).

## 5.2 SYNTHETIC EXPERIMENT WITH RANDOM HIGH DIMENSIONAL DAGS

We randomly draw a graph from the Erdős-Rényi random graph model with a total number of nodes  $p = 20$ . We do rejection sampling to exclude graphs that either contain mediators—as they violate Assumption 3.2—or do not contain at least a confounder. We then

<sup>2</sup>In Appendix C.2, we also present experiments for cases when none of the invariances hold.



432 sample data from the resulting DAG via a linear structural causal model, with the only ex-  
 433 ception being the treatment variable  $T$ , which is generated by additionally applying a sig-  
 434 moid function and then sampling from a Bernoulli distribution. We further post-process the  
 435 graph, adding a post-treatment variable  $X_c = Y + T$  and making unobserved either the par-  
 436 ents of  $T$  or  $Y$  (except common parents), depending on the invariance we want to preserve.  
 437 We apply a random uniform mean and variance shift to all  
 438 the nodes in the graph except for  $T$  and  $Y$  to obtain hetero-  
 439 geneous environments, see Appendix D.1 for further  
 440 details.

441 We present here the results for the setting where the par-  
 442 ents of  $T$  (that are not parents of  $Y$ ) are unobserved,  
 443 please refer to Appendix C.3 for additional experiments  
 444 with the other invariances. We sample 100 different  
 445 DAGs and vary the number of available environments  
 446 while keeping the sample size fixed. In Figure 8, we  
 447 plot the empirical MAE averaged across environments.  
 448 Notably, we observe that across all settings and numbers  
 449 of available environments,  $\hat{\theta}_{\text{insta} \rightarrow \ominus}$  significantly outper-  
 450 forms all the other baselines. Expectedly,  $\hat{\theta}_{\text{irm}}$  fails to sur-  
 451 pass all trivial baselines, even with many environments,  
 452 as it lacks the double robustness property.

### 456 5.3 SEMI-SYNTHETIC EXPERIMENTS: THE IHDP DATASET

457  
 458 The IHDP dataset contains covariates from  $n = 748$  low-  
 459 birth-weight, premature infants enrolled in a home visita-  
 460 tion program designed to improve their cognitive scores  
 461 (Hill, 2011). Instead of using the commonly adopted syn-  
 462 thetic functions from Dorie (2016), we simulate a more  
 463 challenging non-linear version of the dataset inspired by  
 464 Kang & Schafer (2007), better reflecting real-world sce-  
 465 narios. Specifically, we retain the 6 continuous features  
 466 from the original dataset and simulate the outcome  $Y$  and  
 467 treatment assignment  $T$  by randomly sampling complex  
 468 functional forms, such as exponentials and polynomials.  
 469 In addition, we introduce a 2-dimensional synthetic col-  
 470 lider,  $X_c$ , as a linear function of  $T$  and  $Y$ . We generate  
 471 environments using Gaussian mean shifts in both pre-and  
 472 post-treatment features, as well as in *either*  $Y$  or  $T$ , and  
 473 set the number of environments to  $|\mathcal{E}| = 5$ . Finally, to  
 474 make the setting more challenging, we also hide one par-  
 475 ent from either  $Y$  or  $T$ —specifically, from the one that is  
 476 not invariant. Please refer to Appendix D.2 for additional  
 477 experimental details.

478 Figure 4 presents the results. The increased complexity of the non-linear setup leads to reduced  
 479 performance across all methods compared to the linear experiments. Despite this,  $\hat{\theta}_{\ominus}$  and  $\hat{\theta}_{\text{insta} \rightarrow \ominus}$   
 480 continue to outperform the baselines. Consistent with previous experiments,  $\hat{\theta}_{\text{irm}}$  exhibits higher  
 481 MAE when  $Y$  is not invariant across environments, and adjusting for all features ( $\hat{\theta}_{\text{all}}$ ) generally  
 482 results in poor performance. Interestingly,  $\hat{\theta}_{\text{null}}$  performs competitively since the confounders have  
 483 a limited impact on the outcome and treatment assignment in this dataset. Additional experiments  
 484 where the post-treatment feature is either a descendant of the outcome, independent noise, or where  
 485 neither  $T$  nor  $Y$  remains invariant are provided in Appendix C.2, along with experiments including  
 mediators between the treatment and the outcome in Appendix C.1.

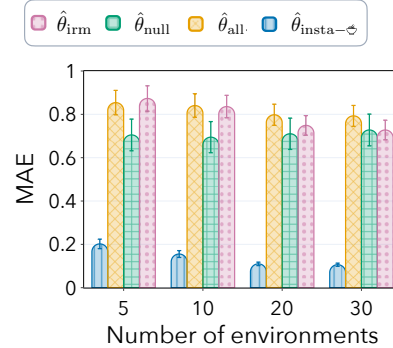


Figure 3: We plot the mean absolute error averaged across environments when the T-invariance is preserved. We sample  $n = 2000$  points for each environment; we report mean and standard error over 100 runs.

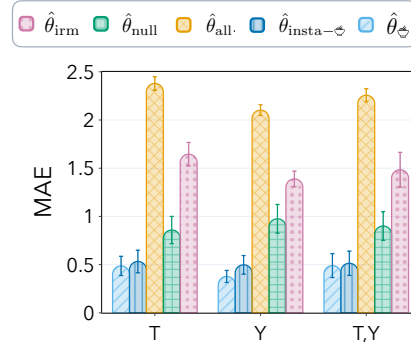


Figure 4: Mean absolute error averaged across environments for the IHDP dataset when different invariances are preserved (T, Y, or both). We consider five environments with  $n = 748$  points each; mean and standard error are reported over 20 runs.

486 5.4 REAL-WORLD EXPERIMENT: EFFECT OF MATERNAL SMOKING ON BIRTH WEIGHT

487  
488 A classic example of bad controls in epidemiology is the birth-weight paradox: researchers observed  
489 higher mortality rates among infants born to smokers compared to non-smokers, but this relation-  
490 ship reversed for low birth-weight infants (Wilcox, 2001). The paradox was resolved by excluding  
491 the post-treatment covariate “birth weight” from the adjustment set, which had introduced collider  
492 bias (Hernández-Díaz et al., 2006). In our experiments, we analyze data from the same context but  
493 instead focus on the effect of smoking on birth weight, as the mortality data is not publicly available.

494  
495 We evaluate our method on the observational dataset from Cattaneo (2010), which studies the effect of  
496 maternal smoking during pregnancy on birth weight ( $n = 4642$ ). We consider 21 covariates from the  
497 original dataset, using as treatment  $T$  a binary feature indicating whether the mother smoked and, as  
498 the outcome  $Y$ , the birth weight in grams. The environment is defined by the trimester of birth, and thus  
499  $|\mathcal{E}| = 4$ . Given the nature of the treatment, we expect that some features are post-treatment, i.e. measured  
500 after the mother started smoking, as noted in Wilcox (2001). We provide complete experimental details in  
501 Appendix D.3.

Table 1: ATE estimates for the Cattaneo2 dataset using different baselines. We report the mean and standard deviation over 100 initializations of the random seed.

Method	ATE (mean $\pm$ std)
$\hat{\theta}_{\text{null}}$	$-275.25 \pm 10^{-5}$
$\hat{\theta}_{\text{all}}$	$-157.55 \pm 10^{-5}$
$\hat{\theta}_{\text{irm}}$	$-182.65 \pm 48.32$
$\hat{\theta}_{\text{insta-}\ominus}$	$-214.60 \pm 25.20$

502  
503 Table 1 presents the results of the differentiable version of our method, alongside various baselines.  
504 While the ground truth ATE is unknown, the effect estimated by adjusting for the set selected by  
505  $\hat{\theta}_{\text{insta-}\ominus}$  aligns with existing epidemiological literature: both observational and interventional stud-  
506 ies (Meyer & Comstock, 1972; Sexton & Hebel, 1984) as well as statistical analyses (Almond et al.,  
507 2005; Cattaneo, 2010) estimate a decrease of 200 to 250 grams in birth weight for infants born  
508 to smoking mothers compared to non-smoking mothers. In contrast,  $\hat{\theta}_{\text{null}}$  overestimates the ATE,  
509 whereas both  $\hat{\theta}_{\text{all}}$  and  $\hat{\theta}_{\text{irm}}$  underestimate it.

510  
511  
512  
513  
514  
515  
516 6 DISCUSSION AND FUTURE WORK

517  
518 In this work, we proposed Robust ATE identification from Multiple ENvironments (RAMEN), a  
519 method that leverages multiple environments to identify the ATE in the presence of post-treatment  
520 and unobserved variables. To the best of our knowledge, we present the first ATE identification  
521 guarantees in this highly relevant, but previously unexplored setting. We introduce a new version  
522 of double robustness which concerns identification instead of estimation: we identify the treatment  
523 effect if either the causal parents of the treatment or those of the outcome are observed.

524  
525 Nevertheless, our method presents several limitations. First, like other kernel-based methods, our  
526 approach suffers from the curse of dimensionality and the computational complexity associated  
527 with kernel matrix computation. Additionally, the requirement for sufficient heterogeneity across  
528 environments may be too stringent in some practical cases. Finally, the combinatorial subset is  
529 computationally demanding, and the Gumbel trick remains a heuristic solution. Addressing any of  
530 these shortcomings would constitute interesting avenues for future work.

531  
532 REFERENCES

533  
534 Avidit Acharya, Matthew Blackwell, and Maya Sen. Explaining causal findings without bias: De-  
535 tecting and assessing direct effects. *American Political Science Review*, 110(3):512–529, 2016.  
536  
537 John Aldrich. Autonomy. *Oxford Economic Papers*, 41(1):15–34, 1989.  
538  
539 Douglas Almond, Kenneth Chay, and David Lee. The costs of low birth weight. *The Quarterly  
Journal of Economics*, 120(3):1031–1083, 2005.

---

540 Martin Arjovsky, Léon Bottou, Ishaan Gulrajani, and David Lopez-Paz. Invariant risk minimization.  
541 *arXiv preprint arXiv:1907.02893*, 2019.

542

543 Dmitry Arkhangelsky and Guido Imbens. Doubly robust identification for causal panel data models.  
544 *The Econometrics Journal*, 25(3):649–674, 2022.

545 Peter Austin. An introduction to propensity score methods for reducing the effects of confounding  
546 in observational studies. *Multivariate Behavioral Research*, 46(3):399–424, 2011.

547

548 Rina Foygel Barber, Mathias Drton, Nils Sturma, and Luca Weihs. Half-trek criterion for identifica-  
549 bility of latent variable models. *The Annals of Statistics*, 50(6):3174–3196, 2022.

550 Reuben Baron and David Kenny. The moderator–mediator variable distinction in social psycho-  
551 logical research: Conceptual, strategic, and statistical considerations. *Journal of Personality and*  
552 *Social Psychology*, 51(6):1173, 1986.

553 Matias Cattaneo. Efficient semiparametric estimation of multi-valued treatment effects under ignor-  
554 ability. *Journal of Econometrics*, 155(2):138–154, 2010.

555

556 Debo Cheng, Jiuyong Li, Lin Liu, Jixue Liu, Kui Yu, and Thuc Duy Le. Causal query in observa-  
557 tional data with hidden variables. *European Conference on Artificial Intelligence*, 2020.

558

559 Debo Cheng, Jiuyong Li, Lin Liu, Kui Yu, Thuc Duy Le, and Jixue Liu. Toward unique and unbiased  
560 causal effect estimation from data with hidden variables. *IEEE Transactions on Neural Networks*  
561 *and Learning Systems*, 34(9):6108–6120, 2022a.

562 Debo Cheng, Jiuyong Li, Lin Liu, Jiji Zhang, Jixue Liu, and Thuc Duy Le. Local search for efficient  
563 causal effect estimation. *IEEE Transactions on Knowledge and Data Engineering*, 2022b.

564

565 Debo Cheng, Jiuyong Li, Lin Liu, Jixue Liu, and Thuc Duy Le. Data-driven causal effect estimation  
566 based on graphical causal modelling: A survey. *ACM Computing Surveys*, 56(5):1–37, 2024.

567 Victor Chernozhukov, Denis Chetverikov, Mert Demirer, Esther Duflo, Christian Hansen, Whitney  
568 Newey, and James Robins. Double/debiased machine learning for treatment and structural para-  
569 meters. *The Econometrics Journal*, 21(1):C1–C68, 2018.

570 Piersilvio De Bartolomeis, Javier Abad, Konstantin Donhauser, and Fanny Yang. Hidden yet quan-  
571 tifiable: A lower bound for confounding strength using randomized trials. *International Confer-*  
572 *ence on Artificial Intelligence and Statistics*, 2024a.

573

574 Piersilvio De Bartolomeis, Javier Abad, Konstantin Donhauser, and Fanny Yang. Detecting critical  
575 treatment effect bias in small subgroups. *Uncertainty in Artificial Intelligence*, 2024b.

576 Xavier De Luna, Ingeborg Waernbaum, and Thomas Richardson. Covariate selection for the non-  
577 parametric estimation of an average treatment effect. *Biometrika*, 98(4):861–875, 2011.

578

579 Ilker Demirel, Edward De Brouwer, Zeshan Hussain, Michael Oberst, Anthony Philippakis, and  
580 David Sontag. Benchmarking observational studies with experimental data under right-censoring.  
581 *arXiv preprint arXiv:2402.15137*, 2024.

582 Vincent Dorie. Npci: Non-parametrics for causal inference. 2016. URL <https://github.com/vdorie/npci>.

583

584 Mathias Drton, Rina Foygel, and Seth Sullivant. Global identifiability of linear structural equation  
585 models. *The Annals of Statistics*, 39(2):865–886, 2011.

586

587 Doris Entner, Patrik Hoyer, and Peter Spirtes. Data-driven covariate selection for nonparametric  
588 estimation of causal effects. *International Conference on Artificial Intelligence and Statistics*,  
589 2013.

590 Zhuangyan Fang and Yangbo He. Ida with background knowledge. *Uncertainty in Artificial Intelli-*  
591 *gence*, 2020.

592

593 Rina Foygel, Jan Draisma, and Mathias Drton. Half-trek criterion for generic identifiability of linear  
structural equation models. *The Annals of Statistics*, pp. 1682–1713, 2012.

---

594 AmirEmad Ghassami, Saber Salehkaleybar, Negar Kiyavash, and Kun Zhang. Learning causal  
595 structures using regression invariance. *Advances in Neural Information Processing Systems*, 2017.  
596

597 Arthur Gretton, Karsten Borgwardt, Malte Rasch, Bernhard Schölkopf, and Alexander Smola. A  
598 kernel two-sample test. *The Journal of Machine Learning Research*, 13(1):723–773, 2012.

599 Yihong Gu, Cong Fang, Peter Bühlmann, and Jianqing Fan. Causality pursuit from heterogeneous  
600 environments via neural adversarial invariance learning. *arXiv preprint arXiv:2405.04715*, 2024.  
601

602 Limor Gultchin, Matt Kusner, Varun Kanade, and Ricardo Silva. Differentiable causal backdoor  
603 discovery. *International Conference on Artificial Intelligence and Statistics*, 2020.

604 Richard Guo, Anton Rask Lundborg, and Qingyuan Zhao. Confounder selection: Objectives and  
605 approaches. *arXiv preprint arXiv:2208.13871*, 2022.  
606

607 Richard Guo, Emilija Perković, and Andrea Rotnitzky. Variable elimination, graph reduction and  
608 the efficient g-formula. *Biometrika*, 110(3):739–761, 2023.

609 Zijian Guo, Hyunseung Kang, Tony Cai, and Dylan Small. Confidence intervals for causal effects  
610 with invalid instruments by using two-stage hard thresholding with voting. *Journal of the Royal  
611 Statistical Society Series B: Statistical Methodology*, 80(4):793–815, 2018.  
612

613 Jinyong Hahn. Functional restriction and efficiency in causal inference. *The Review of Economics  
614 and Statistics*, 86(1):73–76, 2004.

615 Jason Hartford, Victor Veitch, Dhanya Sridhar, and Kevin Leyton-Brown. Valid causal inference  
616 with (some) invalid instruments. *International Conference on Machine Learning*, 2021.  
617

618 Fernando Pires Hartwig, George Davey Smith, and Jack Bowden. Robust inference in summary  
619 data mendelian randomization via the zero modal pleiotropy assumption. *International Journal  
620 of Epidemiology*, 46(6):1985–1998, 2017.

621 Christina Heinze-Deml, Jonas Peters, and Nicolai Meinshausen. Invariant causal prediction for  
622 nonlinear models. *Journal of Causal Inference*, 6(2):20170016, 2018.

623 Leonard Henckel, Emilija Perković, and Marloes Maathuis. Graphical criteria for efficient total  
624 effect estimation via adjustment in causal linear models. *Journal of the Royal Statistical Society  
625 Series B: Statistical Methodology*, 84(2):579–599, 2022.  
626

627 Miguel Hernán and James Robins. *Causal inference*, 2010.

628 Sonia Hernández-Díaz, Enrique Schisterman, and Miguel Hernán. The birth weight “paradox”  
629 uncovered? *American Journal of Epidemiology*, 164(11):1115–1120, 2006.  
630

631 Jennifer Hill. Bayesian nonparametric modeling for causal inference. *Journal of Computational and  
632 Graphical Statistics*, 20(1):217–240, 2011.

633 Biwei Huang, Kun Zhang, Jiji Zhang, Joseph Ramsey, Ruben Sanchez-Romero, Clark Glymour,  
634 and Bernhard Schölkopf. Causal discovery from heterogeneous/nonstationary data. *Journal of  
635 Machine Learning Research*, 21(89):1–53, 2020.  
636

637 Zeshan Hussain, Ming-Chieh Shih, Michael Oberst, Ilker Demirel, and David Sontag. Falsifica-  
638 tion of internal and external validity in observational studies via conditional moment restrictions.  
639 *International Conference on Artificial Intelligence and Statistics*, 2023.

640 Zeshan M Hussain, Michael Oberst, Ming-Chieh Shih, and David Sontag. Falsification before  
641 extrapolation in causal effect estimation. *Advances in Neural Information Processing Systems*,  
642 35, 2022.

643 Antti Hyttinen, Frederick Eberhardt, and Matti Järvisalo. Do-calculus when the true graph is un-  
644 known. *Uncertainty in Artificial Intelligence*, 2015.  
645

646 Kosuke Imai, Luke Keele, Dustin Tingley, and Teppei Yamamoto. Unpacking the black box of  
647 causality: Learning about causal mechanisms from experimental and observational studies. *Amer-  
ican Political Science Review*, 105(4):765–789, 2011.

---

648 Eric Jang, Shixiang Gu, and Ben Poole. Categorical reparameterization with gumbel-softmax. *International Conference on Learning Representations*, 2017.

649

650

651 Nathan Kallus, Aahlad Manas Puli, and Uri Shalit. Removing hidden confounding by experimental

652 grounding. *Advances in Neural Information Processing Systems*, 31, 2018.

653

654 Hyunseung Kang, Anru Zhang, Tony Cai, and Dylan Small. Instrumental variables estimation with

655 some invalid instruments and its application to mendelian randomization. *Journal of the American*

656 *Statistical Association*, 111(513):132–144, 2016.

657 Joseph Kang and Joseph Schafer. Demystifying double robustness: A comparison of alternative

658 strategies for estimating a population mean from incomplete data. *Statistical Science*, pp. 523–

659 539, 2007.

660 Rickard KA Karlsson and Jesse H Krijthe. Detecting hidden confounding in observational data

661 using multiple environments. *Advances in Neural Information Processing Systems*, 37, 2023.

662

663 Ilmun Kim and Aaditya Ramdas. Dimension-agnostic inference using cross u-statistics. *Bernoulli*,

664 30(1):683–711, 2024.

665

666 Gary King. A hard unsolved problem? post-treatment bias in big social science questions. *Hard*

667 *Problems in Social Science Symposium*, 2010.

668 Zhaobin Kuang, Frederic Sala, Nimit Sohoni, Sen Wu, Aldo Córdova-Palomera, Jared Dunnmon,

669 James Priest, and Christopher Ré. Ivy: Instrumental variable synthesis for causal inference. *International Conference on Artificial Intelligence and Statistics*, 2020.

670

671 Marloes Maathuis and Diego Colombo. A generalized back-door criterion. *The Annals of Statistics*,

672 43(3):1060–1088, 2015.

673

674 Marloes Maathuis, Markus Kalisch, and Peter Bühlmann. Estimating high-dimensional intervention

675 effects from observational data. *The Annals of Statistics*, 37(6A):3133–3164, 2009.

676

677 Chris Maddison, Andriy Mnih, and Yee Whye Teh. The concrete distribution: A continuous re-

678 laxation of discrete random variables. *International Conference on Learning Representations*,

679 2017.

680 Daniel Malinsky and Peter Spirtes. Estimating bounds on causal effects in high-dimensional and

681 possibly confounded systems. *International Journal of Approximate Reasoning*, 88:371–384,

682 2017.

683

684 Sarah Mameche, Jilles Vreeken, and David Kaltenpoth. Identifying confounding from causal mech-

685 anism shifts. In *International Conference on Artificial Intelligence and Statistics*, 2024.

686

687 Mary Meyer and George Comstock. Maternal cigarette smoking and perinatal mortality. *American*

688 *Journal of Epidemiology*, 96(1):1–10, 1972.

689

690 Jacob Montgomery, Brendan Nyhan, and Michelle Torres. How conditioning on posttreatment vari-

691 ables can ruin your experiment and what to do about it. *American Journal of Political Science*, 62

692 (3):760–775, 2018.

693

694 Marco Morucci, Vittorio Orlandi, Harsh Parikh, Sudeepa Roy, Cynthia Rudin, and Alexander Vol-

695 fovsky. A double machine learning approach to combining experimental and observational data. *arXiv preprint arXiv:2307.01449*, 2023.

696

697 Michael Oberst, Alexander D’Amour, Minmin Chen, Yuyan Wang, David Sontag, and Steve Yad-

698 lowsky. Understanding the risks and rewards of combining unbiased and possibly biased estima-

699 tors, with applications to causal inference. *arXiv preprint arXiv:2205.10467*, May 2022.

700

701 Judea Pearl. Causal diagrams for empirical research. *Biometrika*, 82(4):669–688, 1995.

Judea Pearl. Direct and indirect effects. *Probabilistic and causal inference: the works of Judea Pearl*, pp. 373–392, 2022.

---

702 Emilija Perković, Markus Kalisch, and Marloes Maathuis. Interpreting and using cpdags with back-  
703 ground knowledge. *Uncertainty in Artificial Intelligence*, 2017.  
704

705 Emilija Perković, Johannes Textor, Markus Kalisch, and Marloes Maathuis. Complete graphical  
706 characterization and construction of adjustment sets in markov equivalence classes of ancestral  
707 graphs. *Journal of Machine Learning Research*, 18(220):1–62, 2018.

708 Jonas Peters, Peter Bühlmann, and Nicolai Meinshausen. Causal inference by using invariant pre-  
709 diction: identification and confidence intervals. *Journal of the Royal Statistical Society Series B: Statistical Methodology*, 78(5):947–1012, 2016.  
710

711 Jonas Peters, Dominik Janzing, and Bernhard Schölkopf. Elements of causal inference: foundations  
712 and learning algorithms. *The MIT Press*, 2017.  
713

714 Niklas Pfister, Peter Bühlmann, and Jonas Peters. Invariant causal prediction for sequential data.  
715 *Journal of the American Statistical Association*, 2019.  
716

717 Niklas Pfister, Evan Williams, Jonas Peters, Ruedi Aebersold, and Peter Bühlmann. Stabilizing  
718 variable selection and regression. *The Annals of Applied Statistics*, 15(3):1220–1246, 2021.  
719

720 Kristopher Preacher and Andrew Hayes. Spss and sas procedures for estimating indirect effects in  
721 simple mediation models. *Behavior research methods, instruments, & computers*, 36:717–731,  
722 2004.

723 James Robins and Sander Greenland. Identifiability and exchangeability for direct and indirect  
724 effects. *Epidemiology*, 3(2):143–155, 1992.  
725

726 James Robins and Andrea Rotnitzky. Semiparametric efficiency in multivariate regression models  
727 with missing data. *Journal of the American Statistical Association*, 90(429):122–129, 1995.

728 James Robins, Andrea Rotnitzky, and Lue Ping Zhao. Estimation of regression coefficients when  
729 some regressors are not always observed. *Journal of the American statistical Association*, 89  
730 (427):846–866, 1994.  
731

732 Mateo Rojas-Carulla, Bernhard Schölkopf, Richard Turner, and Jonas Peters. Invariant models for  
733 causal transfer learning. *Journal of Machine Learning Research*, 19(36):1–34, 2018.

734 Paul Rosenbaum. The consequences of adjustment for a concomitant variable that has been affected  
735 by the treatment. *Journal of the Royal Statistical Society Series A: Statistics in Society*, 147(5):  
736 656–666, 1984.  
737

738 Paul Rosenbaum and Donald Rubin. The central role of the propensity score in observational studies  
739 for causal effects. *Biometrika*, 70(1):41–55, 1983.

740 Elan Rosenfeld, Pradeep Kumar Ravikumar, and Andrej Risteski. The risks of invariant risk mini-  
741 mization. *International Conference on Learning Representations*, 2021.  
742

743 Evan TR Rosenman, Art B Owen, Mike Baiocchi, and Hailey R Banack. Propensity score methods  
744 for merging observational and experimental datasets. *Statistics in Medicine*, 41(1):65–86, 2022.

745 Dominik Rothenhäusler, Peter Bühlmann, and Nicolai Meinshausen. Causal dantzig. *The Annals of*  
746 *Statistics*, 47(3):1688–1722, 2019.  
747

748 Dominik Rothenhäusler, Nicolai Meinshausen, Peter Bühlmann, and Jonas Peters. Anchor regres-  
749 sion: Heterogeneous data meet causality. *Journal of the Royal Statistical Society Series B: Statis-  
750 tical Methodology*, 83(2):215–246, 2021.

751 Andrea Rotnitzky and Ezequiel Smucler. Efficient adjustment sets for population average causal  
752 treatment effect estimation in graphical models. *Journal of Machine Learning Research*, 21(1):  
753 7642–7727, 2020.  
754

755 Mary Sexton and Richard Hebel. A clinical trial of change in maternal smoking and its effect on  
birth weight. *Journal of the American Medical Association*, (7):911–915, 1984.

---

756 Abhin Shah, Karthikeyan Shanmugam, and Kartik Ahuja. Finding valid adjustments under non-  
757 ignorability with minimal dag knowledge. *International Conference on Artificial Intelligence and*  
758 *Statistics*, 2022.

759 Uri Shalit, Fredrik Johansson, and David Sontag. Estimating individual treatment effect: general-  
760 ization bounds and algorithms. *International Conference on Machine Learning*, 2017.

762 Xinwei Shen, Peter Bühlmann, and Armeen Taeb. Causality-oriented robustness: exploiting general  
763 additive interventions. *arXiv preprint arXiv:2307.10299*, 2023.

764 Claudia Shi, Victor Veitch, and David Blei. Invariant representation learning for treatment effect  
765 estimation. *Uncertainty in Artificial Intelligence*, 2021.

767 Ilya Shpitser, Tyler VanderWeele, and James Robins. On the validity of covariate adjustment for  
768 estimating causal effects. *Uncertainty in Artificial Intelligence*, 2010.

769 Arvid Sjölander. Propensity scores and m-structures. *Statistics in medicine*, 28(9):1416–1420, 2009.

771 Ingo Steinwart. On the influence of the kernel on the consistency of support vector machines.  
772 *Journal of Machine Learning Research*, 2:67–93, 2001.

773 Ichiro Takeuchi, Quoc Le, Timothy Sears, Alexander Smola, and Chris Williams. Nonparametric  
774 quantile estimation. *Journal of Machine Learning Research*, 7(7), 2006.

776 Eric Tchetgen Tchetgen and Tyler VanderWeele. Identification of natural direct effects when a  
777 confounder of the mediator is directly affected by exposure. *Epidemiology*, 25(2):282–291, 2014.

778 Tyler Vander Weele and Ilya Shpitser. A new criterion for confounder selection. *Biometrics*, 67(4):  
779 1406–1413, 2011.

781 Stijn Vansteelandt, Tyler VanderWeele, Eric Tchetgen Tchetgen, and James Robins. Multiply robust  
782 inference for statistical interactions. *Journal of the American Statistical Association*, 103(484):  
783 1693–1704, 2008.

784 Haotian Wang, Kun Kuang, Haoang Chi, Longqi Yang, Mingyang Geng, Wanrong Huang, and  
785 Wenjing Yang. Treatment effect estimation with adjustment feature selection. *Conference on*  
786 *Knowledge Discovery and Data Mining*, 2023.

788 Luca Weihs, Bill Robinson, Emilie Dufresne, Jennifer Kenkel, Kaie Kubjas Reginald McGee II,  
789 McGee II Reginald, Nhan Nguyen, Elina Robeva, and Mathias Drton. Determinantal generaliza-  
790 tions of instrumental variables. *Journal of Causal Inference*, 6(1):20170009, 2018.

791 Halbert White and Xun Lu. Causal diagrams for treatment effect estimation with application to  
792 efficient covariate selection. *Review of Economics and Statistics*, 93(4):1453–1459, 2011.

794 Allen Wilcox. On the importance—and the unimportance—of birthweight. *International journal of*  
795 *epidemiology*, 30(6):1233–1241, 2001.

796 Janine Witte, Leonard Henckel, Marloes Maathuis, and Vanessa Didelez. On efficient adjustment in  
797 causal graphs. *Journal of Machine Learning Research*, 21(246):1–45, 2020.

799 Lili Wu and Shu Yang. Integrative  $r$ -learner of heterogeneous treatment effects combining experi-  
800 mental and observational studies. *Conference on Causal Learning and Reasoning*, 2022.

801 Shu Yang, Donglin Zeng, and Xiaofei Wang. Improved inference for heterogeneous treatment effects  
802 using real-world data subject to hidden confounding. *arXiv preprint arXiv:2007.12922*, 2020.

803 Shu Yang, Chenyin Gao, Donglin Zeng, and Xiaofei Wang. Elastic integrative analysis of ran-  
804 domised trial and real-world data for treatment heterogeneity estimation. *Journal of the Royal*  
805 *Statistical Society Series B: Statistical Methodology*, 85(3):575–596, 04 2023.

807 Mingzhang Yin, Yixin Wang, and David Blei. Optimization-based causal estimation from heteroge-  
808 neous environments. *Journal of Machine Learning Research*, 25:1–44, 2024.

809

810  
811  
812  
813  
814  
815  
816  
817  
818  
819  
820  
821  
822  
823  
824  
825  
826  
827  
828  
829  
830  
831  
832  
833  
834  
835  
836  
837  
838  
839  
840  
841  
842  
843  
844  
845  
846  
847  
848  
849  
850  
851  
852  
853  
854  
855  
856  
857  
858  
859  
860  
861  
862  
863

---

## APPENDICES

The following appendices provide deferred proofs, experiment details, and ablation studies.

### TABLE OF CONTENTS

<b>A</b>	<b>Methodology</b>	<b>17</b>
A.1	Discussion of Assumption 3.3 . . . . .	17
A.2	Proof of Theorem 1 . . . . .	18
A.3	Implementation details . . . . .	19
A.3.1	Algorithm 1: Combinatorial search over subsets . . . . .	20
A.3.2	Algorithm 2: Gumbel trick . . . . .	20
<b>B</b>	<b>Extended related work</b>	<b>23</b>
<b>C</b>	<b>Additional experiments</b>	<b>24</b>
C.1	Robustness to mediators . . . . .	24
C.2	Robustness to lack of invariance . . . . .	24
C.3	Additional random graphs experiments . . . . .	25
C.4	Additional semi-synthetic experiments . . . . .	25
C.5	Robustness to small sample size . . . . .	26
C.6	Robustness to violations of Assumption 4.1 . . . . .	26
<b>D</b>	<b>Experimental details</b>	<b>28</b>
D.1	Synthetic experiments . . . . .	28
D.2	Infant Health and Development Program (IHDP) Dataset . . . . .	29
D.3	Cattaneo2 . . . . .	31



## A METHODOLOGY

### A.1 DISCUSSION OF ASSUMPTION 3.3

First, we observe here that Assumption 3.3 is not a minimal “observability” condition on the parents of  $Y$  and  $T$ : in some cases, it might still be possible to find a valid adjustment set via the observed parents of either  $T$  or  $Y$  (or both), although no full set of parents was observed (see e.g. Figure 5). However, in such cases, the valid adjustment set or the corresponding regression function cannot be recovered via invariance methods, since neither  $T$  nor  $Y$  are invariant across environments. Thus, in a way, Assumption 3.3 is a minimal assumption on the DAG if one wants to recover the ATE via invariance of conditional expectations.

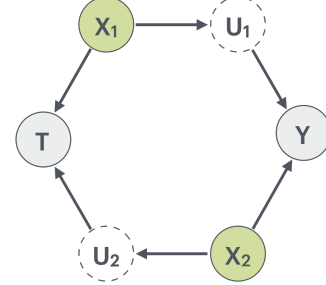


Figure 5: Although neither full set of parents is observed, one can still find a valid adjustment set  $\{X_1, X_2\}$  (in green).

Further, we remark that our assumption is neither stronger nor weaker than the commonly used *ignorability* assumption with respect to  $X$  (Rosenbaum & Rubin, 1983; Robins & Greenland, 1992). For example, if parents of both  $T$  and  $Y$  are unobserved, Assumption 3.3 will not hold, but ignorability could still apply if no *common* parent of  $T$  and  $Y$  is unobserved. Conversely, in graphs with M-bias structures and colliders, the ignorability assumption will not hold.

Below, we give some examples of settings in which Assumption 3.3 holds, including scenarios in the existing invariance literature (Peters et al., 2016; Gu et al., 2024):

**Fully observed DAG** In Peters et al. (2016), we are given multi-environment data  $\{\mathbb{P}^e : e \in \mathcal{E}\}$ , where each distribution  $\mathbb{P}^e$  is induced by an SCM  $\mathcal{M}^e = (\mathcal{G}, \{f_i^e\}_{i=1}^p, \mathbb{P}_\epsilon^e)$ , all variables  $(X_1, \dots, X_d, Y)$  are observed, and for all  $\mathbb{P}^e \in \mathcal{E}$  it is satisfied that

$$Y^e = g(X_{\text{Pa}(Y)}^e, \epsilon^e), \epsilon^e \sim F_\epsilon \text{ and } \epsilon^e \perp\!\!\!\perp X_{\text{Pa}(Y)}^e.$$

In particular, the independence condition implies equality of conditional distributions  $\mathbb{P}^e(Y|X_{\text{Pa}(Y)}^e)$  across environments and thus Assumption 3.3(b).

**General DAG with additive noise** In Gu et al. (2024), the target variable follows the following data generating process for all  $e \in \mathcal{E}$ :

$$Y^e = g(X_{S^*}^e) + \epsilon^e; \quad \mathbb{E}[\epsilon^e | X_{S^*}^e] = 0,$$

where  $S^*$  is the “true important variable set”. This setting is, in a way, more general than Peters et al. (2016), since the noise variable is not required to be independent of the parent variables—instead, the only condition is on the first conditional moment of  $\epsilon^e$ . Due to the additivity of the noise, Assumption 3.3(b) follows immediately.

**General DAG with multiplicative noise** We can define a similar setting for multiplicative noise, setting for all  $e \in \mathcal{E}$ :

$$Y^e = g(X_{S^*}^e)\epsilon^e; \quad \mathbb{E}[\epsilon^e | X_{S^*}^e] = c,$$

where  $S^*$  is, again, the true parent/important variable set, and  $c$  is independent of the environment. We observe that Assumption 3.3(b) follows since it holds that

$$\mathbb{E}^e[Y|X_{S^*}] = \mathbb{E}^e[g(X_{S^*})\epsilon|X_{S^*}] = g(X_{S^*})\mathbb{E}^e[\epsilon|X_{S^*}] = cg(X_{S^*}).$$

**General DAG with polynomial noise** From the above two examples, it becomes clear that for any  $Y = g(X_{S^*})p_k(\epsilon)$ , where  $p$  is a polynomial of degree  $k$ , we have that Assumption 3.3(b) holds if for all  $e \in \mathcal{E}$  it holds that

$$\mathbb{E}^e[\epsilon^{k'} | X_{S^*}] = c_l, \text{ for all } k' \leq k.$$

where  $S^*$  is the important variable/parent set. This condition is strictly weaker than the independence condition since  $k$  is finite.

## A.2 PROOF OF THEOREM 1

First, we establish that the loss function in Equation (6) attains a value of zero at any minimizer  $S_{\text{opt}}$ . By Assumption 3.3, there exists an invariant node  $V \in \{T, Y\}$  whose parents are observed. Since it holds that  $J_{\text{Pa}(V)}(Z; V) = 0$  and  $\text{Pa}(V) \subseteq \mathcal{I}$ , we conclude that there exists a subset  $S \subseteq \mathcal{I}$  such that  $\min\{J_S(Z; T), J_S(Z; Y)\} = 0$ . Additionally, since the loss function is non-negative, any global minimizer of Equation (6) must have a corresponding loss value of zero.

We now consider two cases, depending on whether the minimum is attained for the node  $Y$  or  $T$ . We prove our statement for  $\mathbb{E}_{\mathbb{P}^e}[Y^{\text{do}(T=1)}]$ ; the reasoning is analogous for the control group.

**Case 1:**  $J_{S_{\text{opt}}}(Z; T) = 0$ . Since we assume that the kernel belongs to a universal RKHS (Steinwart, 2001, Def. 4), it follows from Gretton et al. (2012, Theorem 5), that

$$\forall e \in \mathcal{E} : \mathbb{E}_{\mathbb{P}^e}[T \mid X_{S_{\text{opt}}}] = \bar{\pi}(X_{S_{\text{opt}}}), \quad \mathbb{P}^e - \text{a.s.} \quad (8)$$

Then, by Assumption 4.1, it holds that

$$\bar{\pi}(X_{S_{\text{opt}}}) = \bar{\pi}(Z_{\text{Pa}(T)}), \quad \bar{\mathbb{P}} - \text{a.s.}$$

We can now identify the treatment effect using the minimizer of the invariance loss as an adjustment set. First, observe that from Equation (8), for any environment  $e \in \mathcal{E}$ , we have

$$\mathbb{E}_{\mathbb{P}^e} \left[ \frac{TY}{\bar{\pi}(X_{S_{\text{opt}}})} + \left(1 - \frac{T}{\bar{\pi}(X_{S_{\text{opt}}})}\right) \bar{\mu}_1(X_{S_{\text{opt}}}) \right] = \mathbb{E}_{\mathbb{P}^e} \left[ \frac{TY}{\bar{\pi}(Z_{\text{Pa}(T)})} \right] + \mathbb{E}_{\mathbb{P}^e} \left[ \left(1 - \frac{T}{\bar{\pi}(Z_{\text{Pa}(T)})}\right) \bar{\mu}_1(X_{S_{\text{opt}}}) \right].$$

Now, under the positivity assumption and Assumption 3.3, since the parents of  $T$  satisfy the back-door criteria, we can identify the treatment effect, that is, it holds that

$$\mathbb{E}_{\mathbb{P}^e} \left[ \frac{TY}{\bar{\pi}(Z_{\text{Pa}(T)})} \right] = \mathbb{E}_{\mathbb{P}^e} [Y^{\text{do}(T=1)}].$$

It remains to show that the second term is equal to zero:

$$\begin{aligned} \mathbb{E}_{\mathbb{P}^e} \left[ \left(1 - \frac{T}{\bar{\pi}(X_{S_{\text{opt}}})}\right) \bar{\mu}_1(X_{S_{\text{opt}}}) \right] &= \mathbb{E}_{\mathbb{P}^e} [\bar{\mu}_1(X_{S_{\text{opt}}})] - \mathbb{E}_{\mathbb{P}^e} \left[ \frac{T}{\bar{\pi}(X_{S_{\text{opt}}})} \bar{\mu}_1(X_{S_{\text{opt}}}) \right] \\ &= \mathbb{E}_{\mathbb{P}^e} [\bar{\mu}_1(X_{S_{\text{opt}}})] - \mathbb{E}_{\mathbb{P}^e} \left[ \mathbb{E}_{\mathbb{P}^e} \left[ \frac{T}{\bar{\pi}(X_{S_{\text{opt}}})} \mid X_{S_{\text{opt}}} \right] \bar{\mu}_1(X_{S_{\text{opt}}}) \right] \\ &= \mathbb{E}_{\mathbb{P}^e} [\bar{\mu}_1(X_{S_{\text{opt}}})] - \mathbb{E}_{\mathbb{P}^e} [\bar{\mu}_1(X_{S_{\text{opt}}})] \\ &= 0, \end{aligned}$$

where we use the invariance of the conditional expectation  $\pi^e(X_{S_{\text{opt}}})$  for  $e \in \mathcal{E}$  to show that

$$\mathbb{E}_{\mathbb{P}^e} \left[ \frac{T}{\bar{\pi}(X_{S_{\text{opt}}})} \bar{\mu}_1(X_{S_{\text{opt}}}) \mid X_{S_{\text{opt}}} \right] = \bar{\mu}_1(X_{S_{\text{opt}}}).$$

Thus, we conclude that

$$\mathbb{E}_{\mathbb{P}^e} [Y^{\text{do}(T=1)}] = \mathbb{E}_{\mathbb{P}^e} \left[ \frac{TY}{\bar{\pi}(X_{S_{\text{opt}}})} + \left(1 - \frac{T}{\bar{\pi}(X_{S_{\text{opt}}})}\right) \bar{\mu}_1(X_{S_{\text{opt}}}) \right].$$

**Case 2:**  $J_{S_{\text{opt}}}(Z; Y) = 0$ . Again, by the universal property of the kernel  $k$  and Gretton et al. (2012, Theorem 5) it follows that

$$\forall e \in \mathcal{E} : \mathbb{E}_{\mathbb{P}^e}[Y \mid T = t, X_{S_{\text{opt}}}] = \bar{\mu}_t(X_{S_{\text{opt}}}), \quad \mathbb{P}^e - \text{a.s.}, \quad \forall t \in \{0, 1\}.$$

By Assumption 4.1, we have

$$\bar{\mu}_t(X_{S_{\text{opt}}}) = \bar{\mu}_t(Z_{\text{Pa}(Y)}), \quad \bar{\mathbb{P}} - \text{a.s.}$$

972  
973  
974  
975  
976  
977  
978  
979  
980  
981  
982  
983  
984  
985  
986  
987  
988  
989  
990  
991  
992  
993  
994  
995  
996  
997  
998  
999  
1000  
1001  
1002  
1003  
1004  
1005  
1006  
1007  
1008  
1009  
1010  
1011  
1012  
1013  
1014  
1015  
1016  
1017  
1018  
1019  
1020  
1021  
1022  
1023  
1024  
1025

First, observe that

$$\mathbb{E}_{\mathbb{P}^e} [\bar{\mu}_1(X_{S_{\text{opt}}})] = \mathbb{E}_{\mathbb{P}^e} [\bar{\mu}_1(Z_{\text{Pa}(Y)})] = \mathbb{E}_{\mathbb{P}^e} [Y^{\text{do}(T=1)}],$$

since  $Z_{\text{Pa}(Y)}$  is a valid adjustment set.

We then show that the second term in our estimand is zero

$$\begin{aligned} \mathbb{E}_{\mathbb{P}^e} \left[ \frac{(Y - \bar{\mu}_1(X_{S_{\text{opt}}}))T}{\bar{\pi}(X_{S_{\text{opt}}})} \right] &= \mathbb{E}_{\mathbb{P}^e} \left[ \mathbb{E}_{\mathbb{P}^e} \left[ \frac{(Y - \bar{\mu}_1(X_{S_{\text{opt}}}))T}{\bar{\pi}(X_{S_{\text{opt}}})} \mid X_{S_{\text{opt}}} \right] \right] \\ &= \mathbb{E}_{\mathbb{P}^e} \left[ \frac{1}{\bar{\pi}(X_{S_{\text{opt}}})} \mathbb{E}_{\mathbb{P}^e} [(Y - \bar{\mu}_1(Z_{\text{Pa}(Y)}))T \mid X_{S_{\text{opt}}}] \right] \\ &= \mathbb{E}_{\mathbb{P}^e} \left[ \frac{1}{\bar{\pi}(X_{S_{\text{opt}}})} (\mathbb{E}_{\mathbb{P}^e} [YT \mid X_{S_{\text{opt}}}] - \mathbb{E}_{\mathbb{P}^e} [\bar{\mu}_1(Z_{\text{Pa}(Y)})T \mid X_{S_{\text{opt}}}] ) \right] \\ &= \mathbb{E}_{\mathbb{P}^e} \left[ \frac{1}{\bar{\pi}(X_{S_{\text{opt}}})} (\bar{\mu}_1(X_{S_{\text{opt}}})\mathbb{E}_{\mathbb{P}^e} [T \mid X_{S_{\text{opt}}}] - \bar{\mu}_1(X_{S_{\text{opt}}})\mathbb{E}_{\mathbb{P}^e} [T \mid X_{S_{\text{opt}}}] ) \right] = 0, \end{aligned}$$

where we have used the invariance of conditional expectations  $\mu_1^e(X_{S_{\text{opt}}})$  for  $e \in \mathcal{E}$  to show that

$$\begin{aligned} \mathbb{E}_{\mathbb{P}^e} [YT \mid X_{S_{\text{opt}}}] &= \mathbb{E}_{\mathbb{P}^e} [Y \mid X_{S_{\text{opt}}}, T = 1] \mathbb{P}^e(T = 1 \mid X_{S_{\text{opt}}}) \\ &= \mathbb{E}_{\mathbb{P}^e} [\mathbb{E}_{\mathbb{P}^e} [Y \mid T = 1] \mid X_{S_{\text{opt}}}] \mathbb{P}^e(T = 1 \mid X_{S_{\text{opt}}}) \\ &= \mu_1^e(X_{S_{\text{opt}}})\mathbb{P}^e(T = 1 \mid X_{S_{\text{opt}}}) = \mu_1^e(X_{S_{\text{opt}}})\mathbb{E}_{\mathbb{P}^e}[T \mid X_{S_{\text{opt}}}] \\ &= \bar{\mu}_1(X_{S_{\text{opt}}})\mathbb{E}_{\mathbb{P}^e}[T \mid X_{S_{\text{opt}}}], \end{aligned}$$

as well as the fact that for all  $e \in \mathcal{E}$ ,  $\bar{\mu}_1(X_{S_{\text{opt}}}) = \bar{\mu}_1(Z_{\text{Pa}(Y)})$ ,  $\mathbb{P}^e$ -a.s. We now proceed similarly with the remaining two terms: it holds that

$$\mathbb{E}_{\mathbb{P}^e} [\bar{\mu}_0(X_{S_{\text{opt}}})] = \mathbb{E}_{\mathbb{P}^e} [\bar{\mu}_0(Z_{\text{Pa}(Y)})] = \mathbb{E}_{\mathbb{P}^e} [Y^{\text{do}(T=0)}],$$

since  $Z_{\text{Pa}(Y)}$  is a valid adjustment set. We now show that the last remaining term is equal to zero. First, we compute

$$\begin{aligned} \mathbb{E}_{\mathbb{P}^e} \left[ \frac{(Y - \bar{\mu}_0(X_{S_{\text{opt}}})(1 - T))}{1 - \bar{\pi}(X_{S_{\text{opt}}})} \right] &= \mathbb{E}_{\mathbb{P}^e} \left[ \mathbb{E}_{\mathbb{P}^e} \left[ \frac{(Y - \bar{\mu}_0(X_{S_{\text{opt}}})(1 - T))}{1 - \bar{\pi}(X_{S_{\text{opt}}})} \mid X_{S_{\text{opt}}} \right] \right] \\ &= \mathbb{E}_{\mathbb{P}^e} \left[ \frac{1}{1 - \bar{\pi}(X_{S_{\text{opt}}})} \mathbb{E}_{\mathbb{P}^e} [Y - \bar{\mu}_0(X_{S_{\text{opt}}}) - YT + \bar{\mu}_0(X_{S_{\text{opt}}})T \mid X_{S_{\text{opt}}}] \right]. \end{aligned}$$

We compute for the inner term that

$$\begin{aligned} &\mathbb{E}_{\mathbb{P}^e} [Y - \bar{\mu}_0(X_{S_{\text{opt}}}) - YT + \bar{\mu}_0(X_{S_{\text{opt}}})T \mid X_{S_{\text{opt}}}] \\ &= \mathbb{E}_{\mathbb{P}^e} [Y \mid X_{S_{\text{opt}}}] - \bar{\mu}_0(X_{S_{\text{opt}}}) - \mathbb{E}_{\mathbb{P}^e} [Y \mid X_{S_{\text{opt}}}, T = 1] \mathbb{P}^e(T = 1 \mid X_{S_{\text{opt}}}) + \bar{\mu}_0(X_{S_{\text{opt}}})\mathbb{P}^e(T = 1 \mid X_{S_{\text{opt}}}) \\ &= \mathbb{E}_{\mathbb{P}^e} [Y \mid X_{S_{\text{opt}}}, T = 1] \mathbb{P}^e(T = 1 \mid X_{S_{\text{opt}}}) + \mathbb{E}_{\mathbb{P}^e} [Y \mid X_{S_{\text{opt}}}, T = 0] \mathbb{P}^e(T = 0 \mid X_{S_{\text{opt}}}) \\ &\quad - \mathbb{E}_{\mathbb{P}^e} [Y \mid X_{S_{\text{opt}}}, T = 0] - \mathbb{E}_{\mathbb{P}^e} [Y \mid X_{S_{\text{opt}}}, T = 1] \mathbb{P}^e(T = 1 \mid X_{S_{\text{opt}}}) \\ &\quad + \mathbb{E}_{\mathbb{P}^e} [Y \mid X_{S_{\text{opt}}}, T = 0] \mathbb{P}^e(T = 1 \mid X_{S_{\text{opt}}}) = 0, \end{aligned}$$

where again we have used the invariance of the conditional expectations  $\mu_0^e(X_{S_{\text{opt}}})$  and  $\mu_1^e(X_{S_{\text{opt}}})$  across environments.

Combining all four terms, we finally obtain

$$\theta_{\ominus}^e = \mathbb{E}_{\mathbb{P}^e} [Y^{\text{do}(T=1)}] - \mathbb{E}_{\mathbb{P}^e} [Y^{\text{do}(T=0)}].$$

### A.3 IMPLEMENTATION DETAILS

In this section, we describe all the implementation details for our methodology.

**Estimation of the loss function** We have several choices when it comes to estimating our loss function, as there is a trade-off between statistical and computational efficiency. For instance, one can choose the linear time estimator proposed in Gretton et al. (2012, Section 6) or the efficient estimator proposed in Kim & Ramdas (2024) that runs in quadratic time. In this paper, we estimate

$$\mathbb{H}_e^2(S) := \mathbb{E}_{\mathbb{P}^e} \left[ \delta_S(Z; V) k \left( Z_S, \tilde{Z}_S^{\text{os}} \right) \delta_S(\tilde{V}, \tilde{Z}^{\text{os}}) \right]$$

using the cross U-statistic from Kim & Ramdas (2024), defined as

$$\hat{\mathbb{H}}_e^2(S) := \frac{2}{n} \sum_{i=1}^{n/2} h_S(Z_i, V_i),$$

$$\text{with } h_S(Z_i, V_i) := \frac{2}{n} \sum_{j=n/2+1}^n \delta_S(Z_i, V_i) k(Z_{i,S}, Z_{j,S}) \delta_S(Z_j, V_j).$$

Moreover, we would like the two loss functions, i.e.,  $J_Y$  and  $J_T$ , to be on the same scale to avoid any finite sample issues. Therefore, we standardize the cross U-statistic by dividing the empirical variance  $\hat{\sigma} \left( \hat{\mathbb{H}}_e^2(S) \right)$ , i.e. the finite sample estimate of the variance term

$$\sigma^2 \left( \hat{\mathbb{H}}_e^2(S) \right) := \mathbb{E}_{\mathbb{P}^e} \left[ (h_S(Z) - \mathbb{E}_{\mathbb{P}^e} [h_S(Z)])^2 \right].$$

**Choice of kernel** An important issue in practice is the selection of the kernel parameters. We used a Gaussian kernel in all of our experiments. We set the bandwidth of the kernel  $\sigma$  to be the median distance between points  $X$  in the pooled sample—this remains a heuristic similar to those described in Takeuchi et al. (2006), and the optimum kernel choice is an ongoing area of research.

### A.3.1 ALGORITHM 1: COMBINATORIAL SEARCH OVER SUBSETS

We now describe the concrete implementation of our first algorithm.

Since we know that  $T$  is a parent of  $Y$ , we can simplify our loss function to incorporate this knowledge. Let us define the quantity  $\delta_{y,t}(X_S, Y) := Y - \bar{\mu}_t(X_S)$ , where  $\bar{\mu}_t(X_S) := \mathbb{E}_{\mathbb{P}}[Y \mid X_S, T = t]$ . We can rewrite the Y-invariance loss function as follows

$$\min_{S \subseteq [d]} \max_{e \in \mathcal{E}, t \in \{0,1\}} \mathbb{E}_{\mathbb{P}^e} [\delta_{y,t}(Y, X_S) k(X_S, X'_S) \delta_{y,t}(Y', X'_S) \mid T = t].$$

Similarly, we define  $\bar{\pi}(X_S) := \mathbb{E}_{\mathbb{P}}[T \mid X_S]$  and minimize the T-invariance loss function

$$\min_{S \subseteq [d]} \max_{e \in \mathcal{E}} \mathbb{E}_{\mathbb{P}^e} [\delta_t(T, X_S) k(X_S, X'_S) \delta_t(T', X'_S)].$$

where  $\delta_t(X_S, T) := T - \bar{\pi}(X_S)$ .

We explain how to compute the adjustment set explicitly in Algorithm 1, assuming oracle access to the nuisance functions. In practice, nuisance functions can be estimated using the pooled data from all environments.

### A.3.2 ALGORITHM 2: GUMBEL TRICK

To deal with the computational infeasibility of searching over all possible subsets of covariates, we propose a continuous relaxation of the optimization problem that can be efficiently solved using gradient descent. The method involves using Gumbel sampling to create differentiable binary masks for covariate selection, which allows optimization via gradient descent. We present the continuous relaxation in Algorithm 2 for obtaining the invariance loss with respect to the node  $T$ ; the algorithm can be extended analogously to minimize the invariance loss for  $Y_1$  and  $Y_0$ .

1080  
1081  
1082  
1083  
1084  
1085  
1086  
1087  
1088  
1089  
1090  
1091  
1092  
1093  
1094  
1095  
1096  
1097  
1098  
1099  
1100  
1101  
1102  
1103  
1104  
1105  
1106  
1107  
1108  
1109  
1110  
1111  
1112  
1113  
1114  
1115  
1116  
1117  
1118  
1119  
1120  
1121  
1122  
1123  
1124  
1125  
1126  
1127  
1128  
1129  
1130  
1131  
1132  
1133

---

**Algorithm 1** Combinatorial search over subsets ( $\hat{\theta}_\ominus$ )

---

- 1: **Input:** Data  $\{(X_e, Y_e, T_e)\}_{i=1}^{n_e}$ , Nuisance functions:  $\bar{\pi}, \bar{\mu}_0, \bar{\mu}_1$   
2: **for each subset**  $S \subseteq [d]$  **do**  
3:     **for each environment**  $e \in \mathcal{E}$  **do**  
4:         Compute T-invariance loss using dataset  $D^e$ :

$$\hat{J}_S(D^e; T) \leftarrow \frac{4}{n^2} \sum_{i=1}^{n/2} \sum_{j=n/2+1}^n (T_i - \bar{\pi}(X_i))k(X_{i,S}, X_{j,S})(T_j - \bar{\pi}(X_j))$$

$$\hat{J}_S(D^e; T) \leftarrow \frac{\hat{J}_S(D^e; Y_0)}{\widehat{\text{Var}}(\hat{J}_S(D^e; T))}$$

- 5:     Compute Y-invariance loss using dataset  $D^e$  for  $T = 1$ :

$$\hat{J}_S(D^e; Y_1) \leftarrow \frac{4}{n^2} \sum_{i=1}^{n/2} \sum_{j=n/2+1}^n (Y_i - \bar{\mu}_1(X_i))k(X_{i,S}, X_{j,S})(Y_j - \bar{\mu}_1(X_j))$$

$$\hat{J}_S(D^e; Y_1) \leftarrow \frac{\hat{J}_S(D^e; Y_1)}{\widehat{\text{Var}}(\hat{J}_S(D^e; Y_1))}$$

- 6:     Compute Y-invariance loss using dataset  $D^e$  for  $T = 0$ :

$$\hat{J}_S(D^e; Y_0) \leftarrow \frac{4}{n^2} \sum_{i=1}^{n/2} \sum_{j=n/2+1}^n (Y_i - \bar{\mu}_0(X_i))k(X_{i,S}, X_{j,S})(Y_j - \bar{\mu}_0(X_j))$$

$$\hat{J}_S(D^e; Y_0) \leftarrow \frac{\hat{J}_S(D^e; Y_0)}{\widehat{\text{Var}}(\hat{J}_S(D^e; Y_0))}$$

- 7:     **end for**

- 8:     Compute the worst environment losses:

$$\hat{J}_S(T) \leftarrow \max_{e \in \mathcal{E}} J_S(D^e; T), \quad \hat{J}_S(Y_1) \leftarrow \max_{e \in \mathcal{E}} J_S(D^e; Y_1), \quad \hat{J}_S(Y_0) \leftarrow \max_{e \in \mathcal{E}} J_S(D^e; Y_0)$$

- 9:     **end for**

- 10: **Return:**  $S_{\text{opt}} \leftarrow \text{argmin}_S \min(\hat{J}_S(T), \hat{J}_S(Y_1), \hat{J}_S(Y_0))$
-

1134  
1135  
1136  
1137  
1138  
1139  
1140  
1141  
1142  
1143  
1144  
1145  
1146  
1147  
1148  
1149  
1150  
1151  
1152  
1153  
1154  
1155  
1156  
1157  
1158  
1159  
1160  
1161  
1162  
1163  
1164  
1165  
1166  
1167  
1168  
1169  
1170  
1171  
1172  
1173  
1174  
1175  
1176  
1177  
1178  
1179  
1180  
1181  
1182  
1183  
1184  
1185  
1186  
1187

---

**Algorithm 2** Gumbel trick for subset selection ( $\hat{\theta}_{\text{insta-}\ominus}$ )

---

- 1: **Input:** Data  $\{(X_e, Y_e, T_e)\}_{e \in \mathcal{E}}$ , initial temperature  $\tau_{\text{init}}$ , final temperature  $\tau_{\text{final}}$ , anneal interval  $k$ , annealing rate  $\alpha$ , learning rates  $\eta_{\text{gate}}, \eta_{\text{nn}}$ , number of epochs  $n_{\text{epochs}}$
  - 2: Initialize the weights  $w_{\bar{\pi}}, w_{\bar{\mu}_0}, w_{\bar{\mu}_1}$  and neural networks  $\theta_{\bar{\pi}}, \theta_{\bar{\mu}_0}, \theta_{\bar{\mu}_1}$
  - 3: Set temperature  $\tau \leftarrow \tau_{\text{init}}$
  - 4: **for** epoch = 1 to  $n_{\text{epochs}}$  **do**
  - 5:   **if** epoch mod  $k = 0$  **then**
  - 6:     Update temperature:  $\tau \leftarrow \max(\tau_{\text{final}}, \tau \cdot \alpha)$
  - 7:   **end if**
  - 8:   **for each environment**  $e \in \mathcal{E}$  **do**
  - 9:     **for each component**  $j$  **do**
  - 10:      Generate mask:  $G_{1,j}, G_{2,j} \sim \text{Gumbel}(0, 1)$
  - 11:       $B_j(w_{\bar{\pi}}) = \text{sigmoid}\left(\frac{w_{\bar{\pi},j} + G_{1,j} - G_{2,j}}{\tau}\right)$
  - 12:     **end for**
  - 13:     Compute invariance loss for  $T$ :
 
$$\hat{J}_{w_{\bar{\pi}}}(D^e; T) \leftarrow \frac{4}{n^2} \sum_{i=1}^{n/2} \sum_{j=n/2+1}^n (T_i - f_{\theta_{\bar{\pi}}}(X_i, w_{\bar{\pi}})) k(X_{i, w_{\bar{\pi}}}, X_{j, w_{\bar{\pi}}}) (T_j - f_{\theta_{\bar{\pi}}}(X_j, w_{\bar{\pi}}))$$

$$\hat{J}_{w_{\bar{\pi}}}(D^e; T) \leftarrow \frac{\hat{J}_{w_{\bar{\pi}}}(D^e; T)}{\widehat{\text{Var}}(\hat{J}_{w_{\bar{\pi}}}(D^e; T))}$$
  - 14:   **end for**
  - 15:   Aggregate environment losses:
 
$$\hat{J}_{w_{\bar{\pi}}}(T) \leftarrow \frac{1}{n_e} \sum_{e \in \mathcal{E}} \hat{J}_{w_{\bar{\pi}}}(D^e; T)$$
  - 16:   Update gate parameters using gradient descent:
 
$$w_{\bar{\pi}} \leftarrow w_{\bar{\pi}} - \eta_{\text{gate}} \nabla_{w_{\bar{\pi}}} \hat{J}_{w_{\bar{\pi}}}(T)$$
  - 17:   Update neural network parameters using gradient descent:
 
$$\theta_{\bar{\pi}} \leftarrow \theta_{\bar{\pi}} - \eta_{\text{nn}} \nabla_{\theta_{\bar{\pi}}} \hat{J}_{w_{\bar{\pi}}}(T)$$
  - 18: **end for**
  - 19: **Return:**  $S_{\text{opt}} \leftarrow \{i : w_{\bar{\pi},i} > 0\}$
-

1188  
1189  
1190  
1191  
1192  
1193  
1194  
1195  
1196  
1197  
1198  
1199  
1200  
1201  
1202  
1203  
1204  
1205  
1206  
1207  
1208  
1209  
1210  
1211  
1212  
1213  
1214  
1215  
1216  
1217  
1218  
1219  
1220  
1221  
1222  
1223  
1224  
1225  
1226  
1227  
1228  
1229  
1230  
1231  
1232  
1233  
1234  
1235  
1236  
1237  
1238  
1239  
1240  
1241

## B EXTENDED RELATED WORK

We discuss here the different challenges associated with the problem of selecting covariates for treatment effect identification. Our focus is to highlight differences and similarities with our methodology—we leave out the orthogonal problem of statistical efficiency for the sake of clarity, and we refer the reader to Guo et al. (2022); Cheng et al. (2024) for a complete survey of methods.

**Covariate selection with pre-treatment covariates** Several works have relaxed the causal sufficiency assumption, allowing for unobserved variables—as long as they are not confounders—while constraining all observed covariates to be pre-treatment. In this setting, the main challenge is M-bias (Sjölander, 2009), which makes adjusting for the full set of covariates not a viable solution. For instance, EHS (Entner et al., 2013) was one of the first methods to obtain partial identification of treatment effects in this setting, however, at the cost of computational inefficiency. Gultchin et al. (2020) propose a more efficient relaxation for EHS to circumvent the computational inefficiency. Further, several more recent works leverage anchor variables to obtain point identification in a computationally efficient way (Cheng et al., 2020; 2022b; Shah et al., 2022). In contrast, our setting is different since we do not assume that all observed covariates are pre-treatment.

**Covariate selection under causal sufficiency** When all the variables in the causal graph are observed, the only challenge towards identifiability is the presence of post-treatment covariates that can introduce collider bias. Several methods have been proposed to tackle this setting—e.g. IDA (Maathuis et al., 2009) and its variants (Perković et al., 2017; Fang & He, 2020) aim to learn a complete graph from data and then infer a valid adjustment set from it to achieve identifiability. However, they suffer from computational inefficiency since they must first learn the entire causal graph, and they only achieve partial identification. More recently, Shi et al. (2021) consider the setting where multiple environments are available and apply invariant risk minimization (IRM) (Arjovsky et al., 2019) for treatment effect estimation. However, it is widely known that IRM requires many environments—linear in the number of covariates—to generalize well even in the linear regime (Rosenfeld et al., 2021). Finally, Wang et al. (2023) recently proposed a reinforcement learning approach to identify the treatment effect. In contrast, our approach achieves point identification while being computationally efficient and not requiring causal sufficiency.

**Identifiability in linear Gaussian SCMs** When the causal graph is a linear Gaussian SCM, the structure of the causal graph (including the hidden variables) imposes algebraic relations between the entries in the covariance matrix and these relations allow or prevent certain aspects of the observable causal model to be recovered. In this regard, several graphical criteria have been identified for deciding whether, in a given causal graph, a specific causal effect can be identified from the covariance for almost all linear Gaussian SCMs compatible with the graph (Drton et al., 2011; Foygel et al., 2012; Weihs et al., 2018; Barber et al., 2022). In contrast, here we are not assuming neither linearity nor gaussianity, and instead rely on multiple heterogeneous data sources for identification.

**Combining data from multiple environments** Given the challenges associated with estimating treatment effects using non-randomized data, several works propose to detect bias in the treatment effect estimated from observational data by leveraging randomized trials (Yang et al., 2023; Morucci et al., 2023; Hussain et al., 2022; 2023; Demirel et al., 2024; De Bartolomeis et al., 2024b;a), and multiple observational studies (Karlsson & Krijthe, 2023; Mameche et al., 2024). Further, another line of work combines data estimate the bias and correct for it, ultimately leading to a more accurate treatment effect estimate (Kallus et al., 2018; Rosenman et al., 2022; Wu & Yang, 2022; Yang et al., 2020; Oberst et al., 2022).

1242  
 1243  
 1244  
 1245  
 1246  
 1247  
 1248  
 1249  
 1250  
 1251  
 1252  
 1253  
 1254  
 1255  
 1256  
 1257  
 1258  
 1259  
 1260  
 1261  
 1262  
 1263  
 1264  
 1265  
 1266  
 1267  
 1268  
 1269  
 1270  
 1271  
 1272  
 1273  
 1274  
 1275  
 1276  
 1277  
 1278  
 1279  
 1280  
 1281  
 1282  
 1283  
 1284  
 1285  
 1286  
 1287  
 1288  
 1289  
 1290  
 1291  
 1292  
 1293  
 1294  
 1295

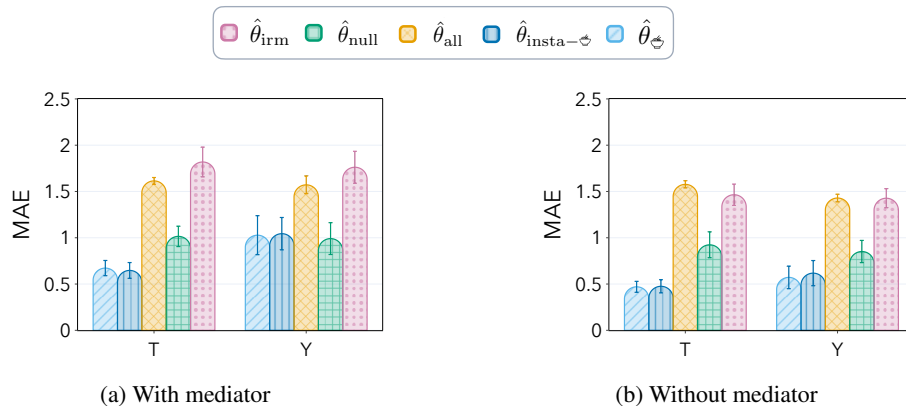


Figure 6: Mean absolute error averaged across environments for the IHDP dataset with a descendant of the outcome  $Y$  when different invariances are preserved ( $T$  or  $Y$ ). We consider the setting with (a) a mediator between  $T$  and  $Y$  and (b) without a mediator. We consider five environments with  $n = 748$  points each; mean and standard error are reported over 20 runs.

## C ADDITIONAL EXPERIMENTS

### C.1 ROBUSTNESS TO MEDIATORS

We study here the robustness of our method to violations of Assumption 3.2. More concretely, we show how the inclusion of a mediator between  $T$  and  $Y$  affects the ATE estimate for our method and the baselines in several settings. We consider the semi-synthetic experiment setup from Section 5.3, using a 2-dimensional descendant of  $Y$  as the post-treatment variable. In Figure 6, we present results for two settings: when the treatment or the outcome is invariant across environments (complete experimental details in Appendix D.2). All baselines show slightly worse performance when a mediator is included. When  $T$  is invariant, our method remains competitive and outperforms the baselines, as the parents of  $T$  still form a valid adjustment set despite the mediator. However, both  $\hat{\theta}_{\rightarrow}$  and  $\hat{\theta}_{insta-\rightarrow}$  experience a significant drop in performance in the  $Y$ -invariance setup, i.e. when  $T$ -invariance is violated. This is expected, as in this scenario, we recover the parents of  $Y$ , which unfortunately also includes the mediator. A closer inspection of the selected subsets reveals that they usually include the mediator, thus failing to estimate the full effect of  $T$  on  $Y$ . Instead, our method recovers the natural direct effect of  $T$  on  $Y$  (Pearl, 2022).

### C.2 ROBUSTNESS TO LACK OF INVARIANCE

Next, we examine the robustness of our method to violations of the invariance in Assumption 3.3. Specifically, we consider again the semi-synthetic experiments of Section 5.3 in the scenario where neither  $T$ - nor  $Y$ -invariance holds and there are post-treatment variables (i.e. not the independent noise setting). We provide the results in Figure 7. The performance of our method significantly worsens in this setting, with performance close to the  $\hat{\theta}_{null}$  baseline, as it often recovers the empty set when no invariant node is present. Nonetheless, our method still outperforms  $\hat{\theta}_{irm}$  in all the settings considered.

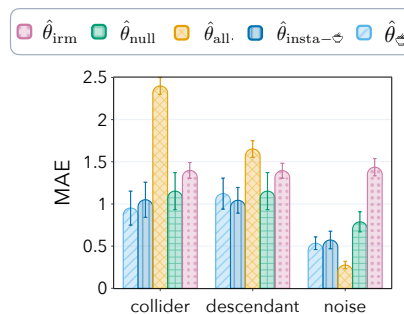


Figure 7: Mean absolute error averaged across environments for the IHDP dataset when no invariance is preserved. We consider five environments with  $n = 748$  points each; mean and standard error are reported over 20 runs.



1296  
1297  
1298  
1299  
1300  
1301  
1302  
1303  
1304  
1305  
1306  
1307  
1308  
1309  
1310  
1311  
1312  
1313  
1314  
1315  
1316  
1317  
1318  
1319  
1320  
1321  
1322  
1323  
1324  
1325  
1326  
1327  
1328  
1329  
1330  
1331  
1332  
1333  
1334  
1335  
1336  
1337  
1338  
1339  
1340  
1341  
1342  
1343  
1344  
1345  
1346  
1347  
1348  
1349

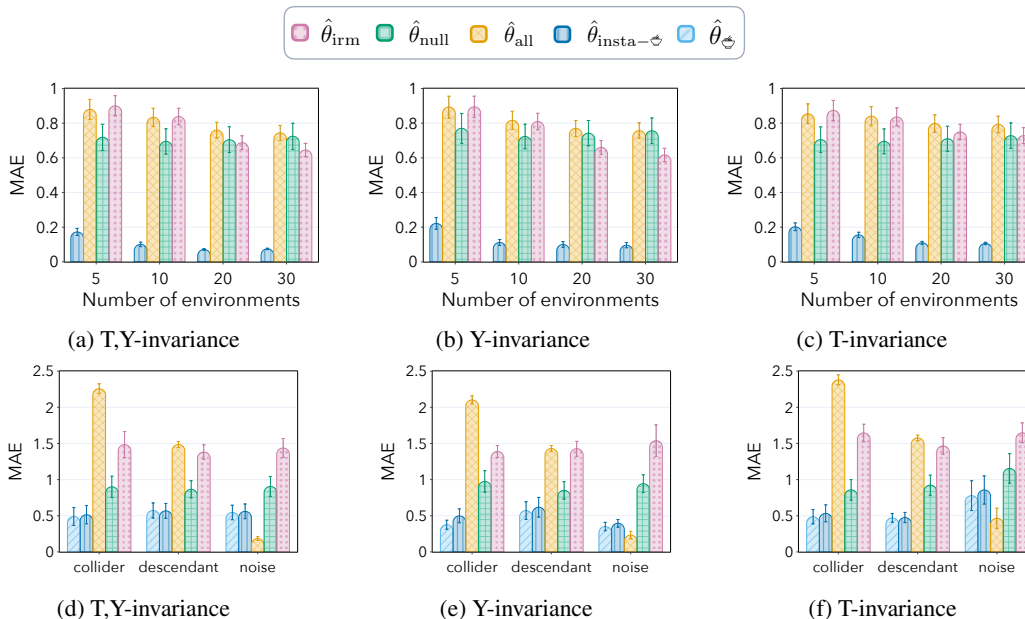


Figure 8: **(Row 1)** We plot the mean absolute error averaged across environments when: (a) no unobserved variables and both invariance w.r.t  $T$  and  $Y$  are preserved; (b) the parents of  $T$  are unobserved but the invariance w.r.t  $Y$  is preserved; (c) the parents of  $Y$  are unobserved but the invariance w.r.t  $T$  is preserved. For all plots, we sample  $n = 2000$  points for each environment; we report mean and standard error over 100 runs. **(Row 2)** Complete experimental results for the semi-synthetic setup described in Section 5.3 using the IHDP dataset. The plots show the mean absolute error averaged across environments for: (a) both  $T$ - and  $Y$ -invariance, (b)  $Y$ -invariance only, (c)  $T$ -invariance only. We consider five environments with  $n = 748$  points each; mean and standard error are reported over 20 runs.

### C.3 ADDITIONAL RANDOM GRAPHS EXPERIMENTS

In Figure 8 (Row 1), we report the MAE averaged across environments for all the invariance settings. First, we observe that across all settings and numbers of available environments, our method significantly outperforms existing baselines. Most notably,  $\hat{\theta}_{\text{insta-}\varnothing}$  achieves relatively small errors even with a limited number of environments. In contrast,  $\hat{\theta}_{\text{irm}}$  requires a much larger number of environments to outperform the trivial baselines  $\hat{\theta}_{\text{null}}$  and  $\hat{\theta}_{\text{all}}$ . Further, when the parents of  $Y$  are unobserved,  $\hat{\theta}_{\text{irm}}$  fails to surpass all trivial baselines, even with many environments—this outcome is expected, as the  $Y$ -invariance is broken in this case and  $\hat{\theta}_{\text{irm}}$  lacks the double robustness.

### C.4 ADDITIONAL SEMI-SYNTHETIC EXPERIMENTS

We present the complete experimental results using the IHDP dataset (see Section 5.3) in Figure 8 (Row 2). Specifically, we evaluate our proposed method and the baselines under three conditions, where the two-dimensional variable  $X_c$  acts as a collider (as described in the main text), descendant, or independent noise. For  $T$ -,  $Y$ -, and  $T, Y$ -invariance, the results align with those obtained in previous sections for linear synthetic experiments. Both  $\hat{\theta}_{\varnothing}$  and its differentiable approximation,  $\hat{\theta}_{\text{insta-}\varnothing}$ , outperform the baselines in most settings. The sole exception is when the post-treatment variables are independent noise, where  $\hat{\theta}_{\text{all}}$  achieves the best performance. In the case of  $T$ -invariance, both our method and  $\hat{\theta}_{\text{irm}}$  exhibit slightly worse performance.  $\hat{\theta}_{\text{irm}}$  generally underperforms, showing the highest error even under the independent noise setting. The  $\hat{\theta}_{\text{null}}$  baseline demonstrates competitive performance overall, likely due to the relatively low influence of confounders in this setup.

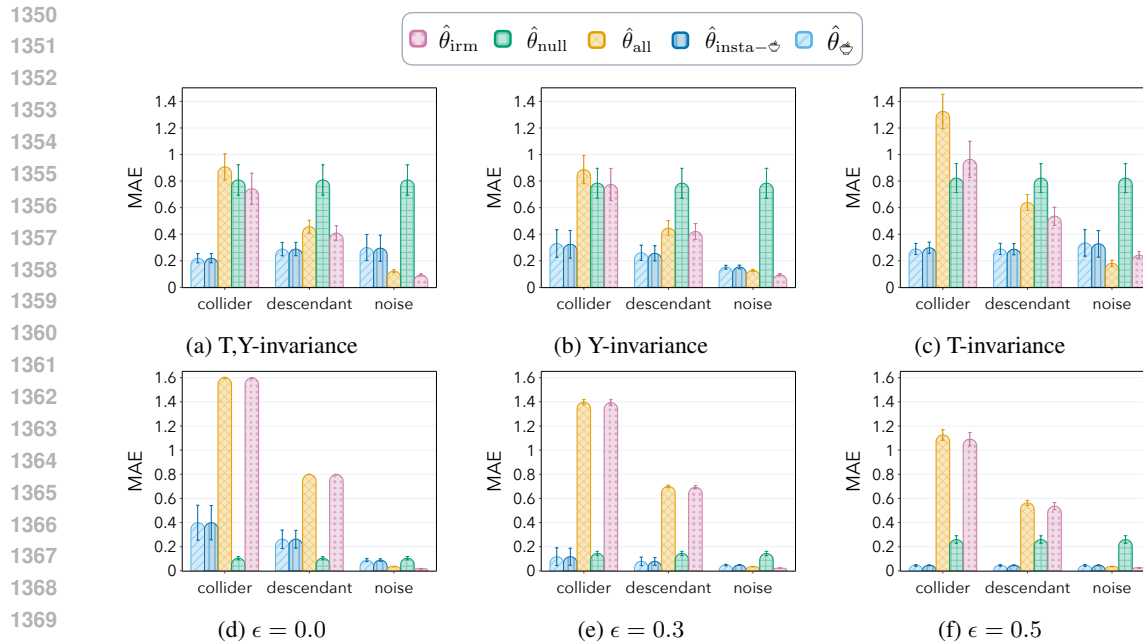


Figure 9: **(Row 1)** For all the plots:  $n = 250$ ,  $d = 3$ ,  $|\mathcal{E}| = 5$ . We plot the mean absolute error averaged across environments when: (a) both invariances are preserved; (b) the invariance w.r.t  $Y$  is preserved; (c) the invariance w.r.t  $T$  is preserved. We report mean and standard error over 20 runs. **(Row 2)** For all the plots:  $n = 2500$ ,  $d = 3$ ,  $|\mathcal{E}| = 5$ , and only the invariant w.r.t  $Y$  is preserved. We plot the mean absolute error averaged across environments for different levels of heterogeneity in the data (higher  $\epsilon$  corresponds to more heterogeneous data).

### C.5 ROBUSTNESS TO SMALL SAMPLE SIZE

In Figure 9 (a–c), we report the MAE averaged across environments for the three graphical models introduced in Figure 2 (Row 2). We can observe that our method remains competitive even in the small sample size regime: our method consistently outperforms all baselines when a collider or descendant is present. However, its performance declines in the edge case where the post-treatment variable is independent noise.

### C.6 ROBUSTNESS TO VIOLATIONS OF ASSUMPTION 4.1

We evaluate here the robustness of our method against violations of our identification condition (i.e. Assumption 4.1). To do so, we slightly modify the synthetic experiments presented in Figure 2: We introduce a parameter  $\epsilon^2$  to control environment heterogeneity. If  $\epsilon^2 = 0$ ,  $X$  has the same distribution across environments. Therefore, there is no heterogeneity across environments, and Assumption 4.1 is violated. On the other hand, if  $\epsilon^2 > 0$ , the mean and variance of  $X$  will shift across environments, with larger shifts as the parameter  $\epsilon^2$  increases. Therefore, the heterogeneity across environments increases with  $\epsilon^2$ , and Assumption 4.1 is more likely to be satisfied.

**Example C.1** (Post-treatment variables). *Let  $\mathcal{E}$  be the collection of environment indices. For each environment  $e \in \mathcal{E}$ , we first sample  $U \sim \mathcal{N}(0, \epsilon^2 I_{d+2})$ . Then, the data is given by*

$$\begin{aligned}
 X_{p,i} &\sim \mathcal{N}(U_i, 0.5 + U_i^2), \text{ for } i = 1, \dots, d; \\
 T &\sim \text{Ber}(\sigma(\beta_t^\top X_p + \epsilon_t)), \text{ with } \beta_t \sim \mathcal{N}(0, I_d) \text{ and } \epsilon_t \sim \mathcal{N}(U_{d+1}, 0.5 + U_{d+1}^2); \\
 Y &= T + \beta_y^\top X_p + \epsilon_y, \text{ with } \beta_y \sim \mathcal{N}(0, I_d) \text{ and } \epsilon_y \sim \mathcal{N}(0, 1); \\
 X_c &= a \cdot T + b \cdot Y + \epsilon_c, \text{ with } \epsilon_c \sim \mathcal{N}(U_{d+2}, 0.5 + U_{d+2}^2).
 \end{aligned}$$

---

1404 In Figure 9 (d–f), we plot the MAE for different levels of heterogeneity in the data. We can observe  
1405 that both  $\hat{\theta}_{\ominus}$  and  $\hat{\theta}_{\text{irm}}$  suffer significantly when there is no heterogeneity ( $\epsilon = 0.0$ ). Nevertheless,  
1406 our method  $\hat{\theta}_{\ominus}$  consistently outperforms  $\hat{\theta}_{\text{irm}}$ , even under strong violations of the identification con-  
1407 dition. Moreover,  $\hat{\theta}_{\ominus}$  remains competitive against all baselines when Assumption 4.1 is only weakly  
1408 satisfied ( $\epsilon = 0.3$ ).  
1409

1410  
1411  
1412  
1413  
1414  
1415  
1416  
1417  
1418  
1419  
1420  
1421  
1422  
1423  
1424  
1425  
1426  
1427  
1428  
1429  
1430  
1431  
1432  
1433  
1434  
1435  
1436  
1437  
1438  
1439  
1440  
1441  
1442  
1443  
1444  
1445  
1446  
1447  
1448  
1449  
1450  
1451  
1452  
1453  
1454  
1455  
1456  
1457

## D EXPERIMENTAL DETAILS

Given an adjustment set, we estimate the ATE for each environment  $e \in \mathcal{E}$  as follows

$$\hat{\theta}_S^e = \frac{1}{n} \sum_{(X_i, T_i, Y_i) \in D^e} \hat{\mu}_S^e(X_i, 1) - \hat{\mu}_S^e(X_i, 0) + \frac{(Y_i - \hat{\mu}_S^e(X_i, 1))T_i}{\hat{\pi}_S^e(X_i)} - \frac{(Y_i - \hat{\mu}_S^e(X_i, 0))(1 - T_i)}{1 - \hat{\pi}_S^e(X_i)},$$

where  $\hat{\mu}_S^e(x, t) = \hat{\mathbb{E}}_{\mathbb{P}^e} [Y \mid T = t, X_S = x]$  and  $\hat{\pi}_S^e(x) = \hat{\mathbb{E}}_{\mathbb{P}^e} [T \mid X_S = x]$ .

For  $\hat{\theta}_{\text{irm}}$ , since the algorithm only learns the outcome function, we estimate the ATE as

$$\hat{\theta}_{\text{irm}} = \frac{1}{n} \sum_{(X_i, T_i, Y_i) \in D^e} \hat{\mu}_S^e(X_i, 1) - \hat{\mu}_S^e(X_i, 0).$$

### D.1 SYNTHETIC EXPERIMENTS

We describe here the data generating process for our synthetic experiments and all the implementation details for the methods.

**Example D.1** (Post-treatment variables). *Let  $\mathcal{E}$  be the collection of environment indices. For each environment  $e \in \mathcal{E}$ , we first sample  $U \sim \mathcal{N}(0, I_{d+2})$ . Then, the data is given by*

$$X_{p,i} \sim \mathcal{N}(U_i, U_i^2), \text{ for } i = 1, \dots, d;$$

$$T \sim \text{Ber}(\sigma(\beta_t^\top X_p + \epsilon_t)), \text{ with } \beta_t \sim \mathcal{N}(0, I_d) \text{ and } \epsilon_t \sim \begin{cases} \mathcal{N}(0, 1) & \text{if } T \text{ is invariant} \\ \mathcal{N}(U_{d+1}, U_{d+1}^2) & \text{else} \end{cases};$$

$$Y = T + \beta_y^\top X_p + \epsilon_y, \text{ with } \beta_y \sim \mathcal{N}(0, I_d) \text{ and } \epsilon_y \sim \begin{cases} \mathcal{N}(0, 1) & \text{if } Y \text{ is invariant} \\ \mathcal{N}(U_{d+1}, U_{d+1}^2) & \text{else} \end{cases};$$

$$X_c = a \cdot T + b \cdot Y + \epsilon_c, \text{ with } \epsilon_c \sim \mathcal{N}(U_{d+2}, U_{d+2}^2).$$

Further, observe that for each choice of invariance, the post-treatment variable  $X_c$  can either be a descendant of  $Y$  ( $a = 0$  and  $b = 1$ ), a collider between  $T$  and  $Y$  ( $a = 1$  and  $b = 1$ ), or independent noise ( $a = 0, b = 0$ ). Finally, under this data-generating process, the average treatment effect is constant across the environments, and it is given by  $\theta^e = 1$ , for all  $e \in \mathcal{E}$ .

**Random graph data generating process** We randomly draw a graph from the Erdős-Rényi random graph model with a density equal to 0.5 and consider graphs with a total number of observed nodes  $p = 20$ . We do rejection sampling to exclude graphs that either contain mediators (since they violate Assumption 3.2) or do not contain at least a confounder (to make the setting more challenging). We then sample data from the resulting DAG via a linear structural causal model with Gaussian weights using the `causal DAG` python library, with the only exception being the treatment variable  $T$ , which is generated by additionally applying a sigmoid function and then sampling from a Bernoulli distribution. We further post-process the graph, adding a post-treatment variable  $X_c = Y + T$  and removing at random some parents of  $T$  or  $Y$  depending on which invariance we want to preserve. Therefore, we consider a challenging scenario with both a collider and unobserved variables. To sample data from multiple environments  $e \in \mathcal{E}$ , within each environment  $e$ , we apply a random uniform mean and variance shift to all the nodes in the graph, except for  $T$  and  $Y$ .

**Implementation details** We implement our method,  $\hat{\theta}_{\text{insta-}\ominus}$ , by performing a hyperparameter search over the following parameters at each iteration: learning rate in the range [0.001, 0.01, 0.1], initial temperature values of [0.5, 0.8, 1.0], and annealing rates of [0.9, 0.95, 0.99]. The optimal combination of these hyperparameters is selected based on minimizing both T-invariance and Y-invariance loss. The outcome functions for  $\hat{\theta}_{\text{all}}$ ,  $\hat{\theta}_{\ominus}$ ,  $\hat{\theta}_{\text{insta-}\ominus}$  and  $\hat{\theta}_{\text{irm}}$  are estimated using a linear regression model. Logistic regression is used for propensity score estimation.

---

## 1512 D.2 INFANT HEALTH AND DEVELOPMENT PROGRAM (IHDP) DATASET

1513  
1514 The Infant Health and Development Program (IHDP) dataset is a randomized controlled trial focusing on low-birth-weight, premature infants. For our analysis, we keep six continuous covariates from Dorie (2016), representing the child’s birth weight, head circumference at birth, number of weeks pre-term, birth order, neonatal health index, and mother’s age at birth.

1518  
1519 Instead of adopting the treatment and outcome functions from Dorie (2016), we simulate a more challenging scenario inspired by Kang & Schafer (2007). In this setting, each covariate assigned to the treatment ( $T$ ) or outcome ( $Y$ ) undergoes a transformation using a predefined set of complex functions similar to those encountered in real-world applications. We introduce the following relationships:

- 1524 • Confounders: Three of the six covariates are randomly selected to act as confounders, affecting both  $T$  and  $Y$ .
- 1525 • Other pre-treatment covariates: The remaining covariates are assigned to affect either  $T$  or  $Y$ , but not both.
- 1526 • Post-treatment covariates: We include a two-dimensional post-treatment covariate, denoted as  $Z$ , whose generation is detailed below.
- 1527 • Environmental variation: To introduce variation across environments, we (i) randomly omit a parent of either  $T$  or  $Y$  and (ii) introduce environment-specific shifts, as detailed below. We apply both to the same node ( $T$  or  $Y$ ) so that the other remains invariant.
- 1528 • We set  $ATE = 2.0$  for all environments.

1531  
1532 **Modeling of  $T$  and  $Y$**  For each covariate  $X_i$  affecting  $T$ , we apply a randomly chosen transformation  $g_T^{(i)}(x)$  from the following set:

$$1533 \quad g_T^{(i)}(x) \in \left\{ 0.5 \log(|x| + 1), \left(\frac{x}{2}\right)^2, x + 0.2, \exp\left(\frac{x}{2}\right) \right\}.$$

1536  
1537 We then compute the logits for the treatment assignment as:

$$1538 \quad T_{\text{logits}} = \sum_i \beta_T^{(i)} g_T^{(i)}(X_i),$$

1539  
1540 where  $\beta_T^{(i)}$  are coefficients sampled independently from a uniform distribution  $\beta_T^{(i)} \sim \mathcal{U}(-0.5, 0.5)$ . The binary treatment  $T$  is obtained by applying a sigmoid function to  $T_{\text{logits}}$  and sampling from a Bernoulli distribution:

$$1541 \quad P(T = 1) = \sigma(T_{\text{logits}}), \quad T \sim \text{Bernoulli}(P(T = 1)),$$

1542  
1543 where  $\sigma(x) = \frac{1}{1+e^{-x}}$  is the sigmoid function.

1544  
1545 Similarly, for each covariate  $X_j$  affecting  $Y$ , we apply a randomly chosen transformation  $g_Y^{(j)}(x)$  from the set:

$$1546 \quad g_Y^{(j)}(x) \in \left\{ 2 \log(|x|), \left(\frac{x}{2}\right)^2, x + 1, \exp\left(\frac{x}{2}\right) \right\}$$

1547  
1548 The outcome  $Y$  is then computed as:

$$1549 \quad Y = \sum_j \beta_Y^{(j)} g_Y^{(j)}(X_j),$$

1550  
1551 with coefficients  $\beta_Y^{(j)}$  sampled from  $\beta_Y^{(j)} \sim \mathcal{U}(-2, 2)$ .

1566 **Incorporating environment-specific shifts** To introduce environment-specific variability, we define  
 1567 a hidden variable  $U$  that modifies the pre-treatment and post-treatment covariates, outcome,  
 1568 and treatment assignment across different environments. The environments are indexed by  $u =$   
 1569  $0, 1, 2, 3, 4$ . For each environment, we introduce shifts dependent on  $u$ .

1570 We first sample coefficients:

$$1571 \beta_{\text{inv}} \sim \mathcal{U}(0.5, 1.0), \quad \beta_X \sim \mathcal{U}(0.5, 1.0).$$

1572 For each environment  $u$ , the shifts are generated as:

$$1573 \Delta_{\text{inv}} = u \cdot \beta_{\text{inv}} + \epsilon_{\text{inv}}, \quad \Delta_X = u \cdot \beta_X + \epsilon_X, \quad \Delta_{\text{post}} = u \cdot \beta_X + \epsilon_{\text{post}},$$

1574 where all  $\epsilon_{\text{inv}}, \epsilon_X, \epsilon_{\text{post}}$  are independently sampled from  $\mathcal{N}(0, 1)$ .

1575 Then, for each environment, the covariates are modified:

$$1576 X = X^0 + \Delta_X,$$

1577 where  $X^0$  represents the original covariate values.

1578 Either  $Y$  or  $T$  is also shifted, depending on the invariance we aim to preserve:

$$1579 \text{ If invariance in } T : Y = Y^0 + \Delta_{\text{inv}}, \quad \text{else if invariance in } Y : T_{\text{logits}} = T_{\text{logits}}^0 + \Delta_{\text{inv}},$$

1580 while we add  $\mathcal{N}(0, 1)$  to the invariant node.

1581 **Generation of post-treatment variables  $X_c$**  For each environment, we generate a two-  
 1582 dimensional post-treatment variable  $X_c$  as follows:

1583 • **Collider:**

$$1584 X_c = Y + T + \epsilon_{\text{post}}, \quad \epsilon_{\text{post}} \sim \mathcal{N}(\Delta_{\text{post}}, I_2).$$

1585 • **Descendant:**

$$1586 X_c = Y + \epsilon_{\text{post}}, \quad \epsilon_{\text{post}} \sim \mathcal{N}(\Delta_{\text{post}}, I_2).$$

1587 • **Independent Noise:**

$$1588 X_c = \epsilon_{\text{post}}, \quad \epsilon_{\text{post}} \sim \mathcal{N}(\Delta_{\text{post}}, I_2).$$

1589 **Inclusion of mediators** In some settings, we introduce an additional mediator variable influenced  
 1590 by  $T$ :

$$1591 \text{ Mediator} = \beta_{\text{med}} \cdot T + \epsilon_{\text{med}}, \quad \beta_{\text{med}} \sim \mathcal{U}(-1.0, 1.0), \quad \epsilon_{\text{med}} \sim \mathcal{N}(0, 1).$$

1592 The outcome  $Y$  is then adjusted:

$$1593 Y = Y + \text{Mediator}.$$

1594 **Summary of data generation process** For each environment:

- 1595 1. Modify covariates:  $X = X^0 + \Delta_X$ .
- 1596 2. Compute treatment:  $T_{\text{logits}} = \sum_i \beta_T^{(i)}, g_T^{(i)}(X_i) \quad T \sim \text{Bernoulli}(\sigma(T_{\text{logits}}))$ .
- 1597 3. Compute outcome:  $Y = \sum_j \beta_Y^{(j)}, g_Y^{(j)}(X_j)$ .
- 1598 4. Apply environmental shift to  $Y$  or  $T$  and hide a parent of  $Y$  or  $T$  (we hide the same parent  
 1599 for all environments).
- 1600 5. Include the ATE = 2.0 in the outcome  $Y$
- 1601 6. If applicable, generate mediator and adjust  $Y$ .
- 1602 7. Generate post-treatment variables  $Z$ .

---

1620 **Implementation details** We implement our method,  $\hat{\theta}_{\text{insta-}\varnothing}$ , by performing a hyperparameter  
1621 search over the following parameters at each iteration: learning rate in the range [0.001, 0.01, 0.1],  
1622 initial temperature values of [0.5, 0.8, 1.0], and annealing rates of [0.9, 0.95, 0.99]. The optimal  
1623 combination of these hyperparameters is selected based on the minimization of both T-invariance  
1624 and Y-invariance loss. The outcome and treatment assignment functions for both  $\hat{\theta}_{\text{all}}$  and  $\hat{\theta}_{\text{insta-}\varnothing}$   
1625 are estimated using XGBoost. For these models, we set the number of estimators to 1,000, the  
1626 learning rate to 0.01, and the maximum tree depth to 6. For the non-linear IRM baseline, we employ  
1627 the TARNet architecture (Shalit et al., 2017), which consists of a shared representation with a single  
1628 hidden layer of 200 neurons, followed by two hypothesis-specific hidden layers, each with 100  
1629 neurons. Logistic regression is used for propensity score estimation.

1630

### 1631 D.3 CATTANEO2

1632

1633 The Cattaneo2 dataset (Cattaneo, 2010) studies the effect of maternal smoking on newborn birth  
1634 weight. We consider 21 covariates, including maternal and paternal age and education, marital  
1635 status, maternal foreign status, Hispanic origin, alcohol consumption, receipt of prenatal care and  
1636 the number of prenatal visits, whether the mother had previous children who died, an indicator for  
1637 low birth weight, months since last birth by the mother, birth month, indicator for whether the baby  
1638 is first-born, and other variables for which full details are unavailable. The treatment is a binary  
1639 indicator of smoking status, with 864 mothers in the treatment group and 3,778 in the control group.  
1640 The outcome is a continuous variable representing birth weight, which we normalize to the interval  
1641 [0, 1]. We exclude the month of birth from the observed features and instead use it to define the  
1642 environments, creating four environments corresponding to the four quarters of the year.

1643

1644 **Implementation details** We implement our method,  $\hat{\theta}_{\text{insta-}\varnothing}$ , using the following hyperparame-  
1645 ters: the number of epochs is set to 700, patience to 100, learning rate to 0.1, initial temperature  
1646 to 1.0, and annealing rate to 0.9. This configuration was chosen because it provided robust and fa-  
1647 vorable results across experiments, specifically in minimizing T- and Y-invariance losses. All other  
1648 hyperparameters are kept from previous experiments. The outcome and treatment assignment func-  
1649 tions for both  $\hat{\theta}_{\text{all}}$  and  $\hat{\theta}_{\text{insta-}\varnothing}$  are estimated using XGBoost, with the number of estimators set to  
1650 1,000, learning rate to 0.01, and maximum depth to 6. For the non-linear IRM implementation, we  
1651 use the TARNet architecture, as in the IHDP experiments.

1652

1653

1654

1655

1656

1657

1658

1659

1660

1661

1662

1663

1664

1665

1666

1667

1668

1669

1670

1671

1672

1673